The Openwind Deep-Array Wake Model

Development and validation

Authors:

Nicholas M. Robinson, Director of Openwind®

Beanán O'Loughlin, Global Technical Lead – Wind Energy

Update: July, 2024

Issue: A

Safety. Science. Transformation.™

Notice to third parties

This report was prepared by UL Services Group LLC (“UL Solutions”) and is based on information not within the control of UL Solutions. UL Solutions has assumed the information provided by others, both verbal and written, is complete and correct. While it is believed the information, data and opinions contained herein will be reliable under the conditions and subject to the limitations set forth herein, UL Solutions does not guarantee the accuracy thereof. Use of this report or any information contained therein by any party other than the intended recipient or its affiliates, shall constitute a waiver and release by such third party of UL Solutions from and against all claims and liability, including, but not limited to, liability for special, incidental, indirect or consequential damages in connection with such use. In addition, use of this report or any information contained herein by any party other than the intended recipient or its affiliates, shall constitute agreement by such third party to defend and indemnify UL Solutions from and against any claims and liability, including, but not limited to, liability for special, incidental, indirect or consequential damages in connection with such use. To the fullest extent permitted by law, such waiver and release, and indemnification shall apply notwithstanding the negligence, strict liability, fault, breach of warranty or breach of contract of UL Solutions. The benefit of such releases, waivers or limitations of liability shall extend to the related companies and subcontractors of any tier of UL Solutions, and the directors, officers, partners, employees and agents of all released or indemnified parties.

Table of contents

1. Introduction 1
2. Theoretical Background 2
3. Implementation of Openwind 3
3.1 Mesoscale Modeling 3
3.2 IBL Growth 4
3.3 Blending with the EV Model 5
4. Aim 5
5. Test Method 5
6. Eddy Viscosity Near wake filter 7
7. Offshore Results 11
7.1 Offshore Test Sites 11
7.1.1 Offshore Test Site 1 11
7.1.2 Offshore Test Site 2 12
7.1.3 Offshore Test Site 3 13
7.1.4 Offshore Test Site 4 (Egmond An Zee) 14
7.1.5 Offshore Test Site 5 15
7.2 Orsted Offshore Wake Bench 16
7.3 Offshore Conclusions 18
8. Onshore Results 20
8.1 Onshore Test Sites 20
8.1.1 Onshore Test Site 1 20
8.1.2 Onshore Test Site 2 21
8.1.3 Onshore Test Site 3 22
8.1.4 Onshore Test Site 4 23
8.1.5 Onshore Test Site 5 24
8.1.6 Onshore Test Site 6 25
8.1.7 Onshore Test Site 7 26
8.1.8 Onshore Test Site 8 27
8.1.9 Onshore Test Site 9 28
8.1.10 Onshore Test Site 10 29
8.1.11 Onshore Test Site 11 30
8.1.12 Onshore Test Site 12 31
8.1.13 Onshore Test Site 13 32
8.2 Onshore Conclusions 34
9. Summary 36
Appendix A 38

1. Introduction

In the past several years, researchers have become aware that the current generation of wake models may underestimate wake losses in large wind projects with multiple rows of wind turbines. The crux of the problem is that the leading wake models — including the Park, Modified Park, and Eddy Viscosity (EV) models — ignore two-way interactions between the atmosphere and the turbines.[1] Each turbine extracts energy from the wind passing through its rotor plane, creating a zone of reduced speed extending some distance downstream. Upstream and outside this zone of influence, it is assumed the ambient wind is unaffected.

Both theory and experiments suggest that, for large arrays of wind turbines, this assumption does not hold. The presence of numerous large wind turbines in a limited area can alter the wind profile in the planetary boundary layer outside the zone of direct wake effect, both within and around the array, thereby reducing the amount of energy available to the turbines for power production. Experimental data supporting this hypothesis comes mainly from offshore wind projects, where the contrast between the drag induced by the turbines and the relatively low roughness of the ocean surface makes the so-called deep-array effect especially pronounced. Onshore, the effect is attenuated but theory suggests it may nonetheless be significant in projects involving hundreds to thousands of wind turbines.

It has become clear new models are required that can simulate deep-array wake effects with reasonable accuracy. Predicting the overall impact of a large wind turbine array is a complex problem involving dynamic interactions between the turbines and various properties of the atmosphere, including vertical and horizontal gradients of temperature, pressure, speed and turbulence. This problem can be solved completely only through sophisticated numerical modeling requiring very large computer resources. However, it may be hoped that simplified approaches will work well enough for the purpose of designing and estimating the energy production of the next generation of wind energy projects.

This paper describes a deep-array wake model (DAWM) developed by UL Solutions and implemented in the Openwind plant design and optimization program. The paper discusses the theoretical background of the approach, its specific application in DAWM, and validation of the model at five offshore and 13 onshore wind farms where operational turbine output data are available.

[1] Frandsen, S.T., Barthelmie, R.J., Pryor, S.C., Rathmann, O., Larsen, S. Højstrup, J. and Thøgersen, M. 2006: Analytical Modeling of Wind Speed Deficit in Large Offshore Wind Farms. *Wind Energy*, 9, 39-53.

2. Theoretical Background

The approach taken is based on a theory advanced by Sten Frandsen,[2] in which an infinite array of wind turbines is represented as a region of uniform high surface roughness. The roughness imposes drag on the atmosphere, causing a downstream change in the structure of the planetary boundary layer (PBL) and, in particular, a reduction in the freestream wind speed at the turbine hub height. According to this theory, the wind-farm equivalent roughness z_{00} is given by

$$z_{00} = h_H \exp\left(-\frac{K}{\sqrt{c_t + \left(K/\ln\left(h_H/z_0\right)\right)^2}}\right)$$

Equation 1: wind farm equivalent roughness

In this equation, h_H is the hub height, κ is the von Karman constant (about 0.4), z_0 is the ambient roughness between turbines, and c_t is the distributed thrust coefficient,

$$c_t = \frac{\pi}{8 s_d s_c} C_T$$

Equation 2: distributed thrust coefficient

Here, C_T is the turbine thrust coefficient and s_d and s_c are the mean downwind and crosswind spacings in rotor diameters (RDs). The chart on the left in Figure 1 shows z_{00} for a range of C_T and mean array spacings $(s_d s_c)^{0.5}$. The roughness is strongly dependent on the spacing, much less so on the background or ambient roughness (here assumed to be 0.001 m for offshore arrays and 0.03 m for onshore arrays).

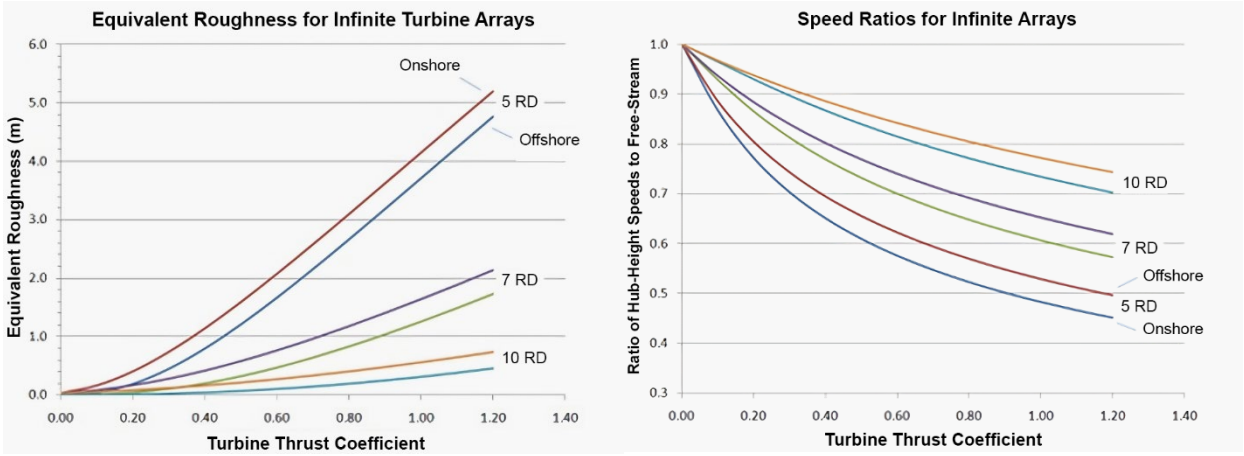

Figure 1: equivalent roughness and waked speed ratios for infinite arrays

[2] Sten Tronæs Frandsen, *Turbulence and Turbulence-Generated Structural Loading in Wind Turbine Clusters*, Risø-R-1188(EN), Risø National Laboratory (January 2007).

Left: Wind farm equivalent roughness z00 for an infinite turbine array as a function of thrust coefficient and array spacing in RDs, for both offshore (ambient z_0=0.001 m) and onshore (ambient z_0=0.03 m) projects.

Right: Asymptotic hub-height wind speed as a fraction of the freestream speed for the same cases. [Based on Frandsen (2007).]

Once the equivalent roughness is defined, the impact on the hub-height wind speed deep within the array (i.e., where the PBL has reached equilibrium with the array roughness) is estimated from meteorological theory under the assumption of a constant geostrophic wind speed *G* and a neutral logarithmic profile throughout the PBL. The result is approximated by the following equation:

$$\frac{v'_H}{v_H} = \left(\frac{z_{00}}{z_0}\right)^{0.07} \frac{\ln\left(h_H/z_{00}\right)}{\ln\left(h_H/z_0\right)}$$

Equation 3: hub-height wind speed deep within array

Here, v'_H and v_H are the hub-height speeds deep within the array and far upstream, respectively. The results are plotted in the right-hand chart in Figure 1.

3. Implementation of Openwind

An important issue with the Frandsen theory is that it does not address the wake effects of individual turbines. Instead, it treats the array as an infinite sea of undifferentiated surface drag. This means that the predicted wind resource at a particular location does not depend on whether there are any turbines immediately upwind or not, which is unrealistic. Furthermore, the roughness depends on the array density which implies it would have to be recalculated every time the layout is modified. Thus, to be useful for wind project design and optimization, the Frandsen theory must either be modified or combined in some way with other methods.

In the course of this research UL Solutions developed and tested a number of different methods of addressing these two issues. The methods fall into two categories: one based on numerical mesoscale weather modeling and the other on empirical equations describing the growth of internal boundary layers (IBLs) at roughness changes.

3.1 Mesoscale Modeling

This approach relies on a mesoscale numerical weather prediction model to simulate the roughness effect. It is hypothesized that this might produce superior results because the model is capable of simulating the impact of roughness changes under a range of atmospheric conditions, most notably thermal stability. The MASS model (Mesoscale Atmospheric Simulation System) was run at a relatively high resolution of 300 m for a representative sample of 72 days. Each grid cell coinciding with a turbine was assigned an increased surface roughness value. The results of the simulations were then used to produce a wind resource grid (WRG) file. Finally, this file was loaded into Openwind for energy production calculations.

After testing at two sites (one offshore, one onshore), it was concluded that the mesoscale modeling approach offers no substantial improvement over the IBL-growth approach at two sites. Furthermore, it

would be impractical to implement it for layout optimization because each new layout would require a new set of mesoscale runs. For these reasons, it was decided not to implement this approach for the time being.

3.2 IBL Growth

The second approach is implemented entirely in Openwind and relies on equations describing the downstream effects of roughness changes on wind speed.[3] Each turbine is assumed to occupy a discrete area of increased surface roughness. As the wind reaches a turbine, an IBL is created by the increased roughness. Within this IBL, the wind profile, or shear, is defined by the turbine roughness rather than by the ambient roughness, with the constraint that the speed at the top of the IBL must match the speed immediately above it. After the wind has passed the turbine, a second IBL is created to represent the transition back to ambient surface conditions. Both IBLs grow with distance downstream according to the following equation[4]:

$$h_{ibl}\left[\ln\left({}^{h_{ibl}}/_{z_0}\right)-1\right]=\left({}^{x}/_{z_0}-1\right)z_0$$

Equation 4: IBL growth with distance

Here, x is the distance from where the IBL is created, and z_0 is the downstream roughness (for the first IBL, the turbine roughness, and for the second, the ambient roughness). Subsequent turbines create their own IBL pairs underneath the previous ones.

Considering just the first turbine's IBL pair, and assuming both IBLs have grown to exceed hub height, the equation for the adjusted hub-height speed is as follows:

$$\frac{v'_H}{v_H}=\frac{\ln\left({}^{h_1}/_{z_0}\right)\ln\left({}^{h_2}/_{z_{00}}\right)}{\ln\left({}^{h_2}/_{z_0}\right)\ln\left({}^{h_1}/_{z_{00}}\right)}$$

Equation 5: Adjusted hub-height speed

Here, h_1 and h_2 are the heights of the first and second IBLs, respectively. This is easily generalized to IBL pairs from multiple turbines. Any IBL that has not attained hub height is assumed to have no impact on the hub-height speed, and any IBL that exceeds the height of a previous IBL supersedes the previous IBL.

After some experimentation, it was decided that the first IBL for each turbine would be initialized at the height of the top of the turbine rotor while the second would be initialized at the bottom of the rotor. This is physically reasonable considering that turbines act not at the surface but across the rotor plane. Effectively it gives the IBLs a head start and allows the large-array effect to develop more rapidly. (The height settings can be varied; those described are the defaults.)

[3] This approach is conceptually similar to the approach taken by Garrad Hassan in its large-array wake model, part of the Wind farmer software package. However, the methods differ in many details.

[4] J.R. Garratt, *The Atmospheric Boundary Layer*, Cambridge University Press (1992), p. 111.

3.3 Blending with the EV model

The IBL-growth approach has the important advantage that it runs fast and, therefore, can be applied easily in an array-optimization procedure. It also varies the wake impact depending on the locations of upstream turbines. Thus, it represents something of a cross between a conventional wake model and Frandsen's theoretical approach.

Still, because its effect depends on the gradual growth of the IBL, the method underestimates the immediate downstream wake impact of individual turbines. For this reason, it must be combined in some way with another wake model to provide a complete picture of the wake effects throughout the array.

Two methods of solving this problem were developed and tested. In the first, the IBL equations modify the freestream wind speeds that are input to the EV model. In the second, the net output of each turbine is estimated separately (i) with the EV model alone (roughness effect switched off), and (ii) with the roughness effect alone (EV model switched off). The two results are then compared and the one predicting the largest wake deficit is retained. This approach implicitly divides the array into two parts: a "shallow zone" where the conventional wake model applies, and a "deep" zone where the roughness effects become dominant. In tests, the dividing line between zones typically occurs about three rows into a wind project.

Tests indicated that the maximum-deficit method appears to have an edge in both accuracy and ease of implementation. Therefore, this approach was adopted in DAWM.

4. Aim

The purpose of this update is to determine the best set of wake modeling settings to apply to the DAWM EV model in order to adequately predict wake losses in both onshore and offshore wind farms. The purpose here is to recommend wake model settings that can be easily and quickly applied and that will give consistent results, whether using frequency domain energy capture (FDEC) or time-series energy capture (TSEC). For these reasons, neither atmospheric stability in the form of the Monin-Obukhov Length (MOL) nor the option to link turbine roughness to thrust coefficient were considered. Another reason for not considering atmospheric stability, even though the DAWM can respond to changes in MOL, is the questionable behavior of Frandsen-style wake models in response to changes in MOL.[5]

5. Test Method

Turbine production data and wind speed and direction data were acquired for five offshore and thirteen onshore wind projects. With minor variations, the same method was applied to all sites to compare the accuracy of the DAWM EV model. The main measure of model accuracy is the mean error (ME) calculated over all turbines for which data are available and the driving met mast is un-waked. The error is defined as the modeled wake loss minus observed wake loss as a percentage of the observed wake loss. The observed wake loss is inferred by scaling the supervisory control and data acquisition (SCADA) production data to match the modeled production in the front row (un-waked) turbines. This is intended to remove any issues with turbine performance as well as differences between the published and actual power curves of the turbines. Clearly, this method is somewhat confounding if one wishes to fully investigate global blockage effects. This is beyond the scope of this paper and will be addressed in upcoming updates.

The modeled production was computed in time-series mode before being compiled into bins by direction and wind speed. This approach avoids the need to filter the data beforehand while allowing the use of time-

[5] Peña & Rathman, *Atmospheric stability-dependent infinite wind-farm models and the wake-decay coefficient*, (2014).

varying inputs in addition to wind speed and direction such as MOL,[6] turbulence intensity, temperature, density, atmospheric boundary layer[6] height and so on.

While the Rankine Half-Body (RHB) induction model proposed by Gribben[7] does not take account of atmospheric stability, turbulence intensity or atmospheric boundary layer (ABL) height, and therefore does not attempt to model the global blockage effect, it was chosen in order to include some measure of the local induction effects.

The use of overall ME metric in the tuning of the wake model parameters is in line with UL Solutions backcast methodology in which the focus is primarily on achieving a zero mean bias and, secondarily, but also importantly, decreasing the spread of individual project biases around that zero mean bias. The root mean squared error (RMSE) is easily computable for any model to data comparison and represents a combination of bias and uncertainty ($RMSE^2$=$bias^2$+standard $deviation^2$) as when the overall mean bias is zero, the standard deviation of the errors represents the uncertainty. A mean bias of zero does not necessarily mean the model is doing a good job of modeling the phenomenon of interest (in this case array losses). It simply means that over a number of tests, the positive and negative errors canceled out. The use of squared error in RMSE does not allow positive and negative errors to cancel each other and emphasizes larger errors over smaller ones. The RMSE can still be high even when the bias is zero and so the RMSE can be used to assess how well the data is being modeled. For two wake model configurations, both with zero or near zero bias, the one with the lower RMSE can be thought of as doing a better job of modeling the variation in the array losses.

The results in Section 7 and Section 8 present the performance of these error metrics, as well as a graphical presentation of the radial modeled and operational wakes. Unless otherwise stated in the graphs, innermost rings represent the 5m/s bin, and the outermost rings represent the 13m/s bin with white cells representing directions in which usable SCADA data was unavailable for the front row turbines, e.g., Figure 6.

[6] Not used in this study.

[7] Brian J Gribben and Graham S Hawkes (2019) Technical Paper: A potential flow model for wind turbine induction and wind farm blockage. Frazer-Nash Consultancy.

6. Eddy Viscosity Near wake filter

In previous implementations of the DAWM EV, the Near wake filter (NWF) was enabled. Evidence arising from this validation study suggested that the NWF being enabled resulted in an over-prediction of in-line wakes for more closely spaced turbines. The disabling of the NWF resulted in improved wake modeling relative to the operational data.

Examples of the improved performance without the NWF are shown in Figure 2 to Figure 4 below. As can be seen when comparing the modeled and operational efficiencies by row, enabling the near wake filter significantly over-estimates the wake effects in this case when the wind is directly along the rows of turbines.

Please note that the wake rows are determined automatically using the current wake model settings and so different wake model settings will result in different turbines being assigned to any given row. Hence, the operational efficiencies per row will change somewhat from run to run.

It was decided to remove the near wake filter as standard for both on and offshore modeling and all results presented in Section 7 and Section 8 are representative of this setting.

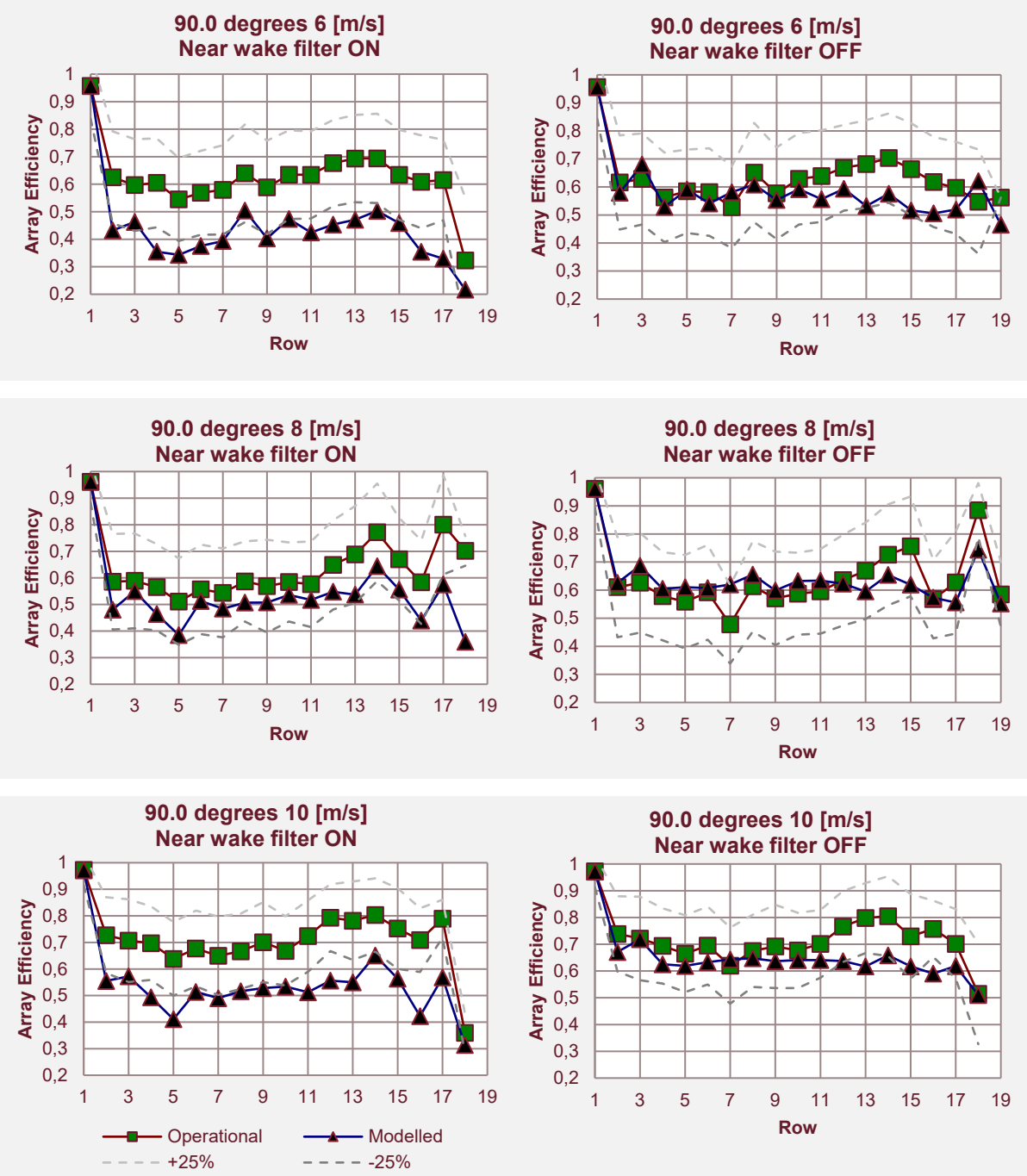

Figure 2: Effects of enabling and disabling the EV near wake filter – Example 1

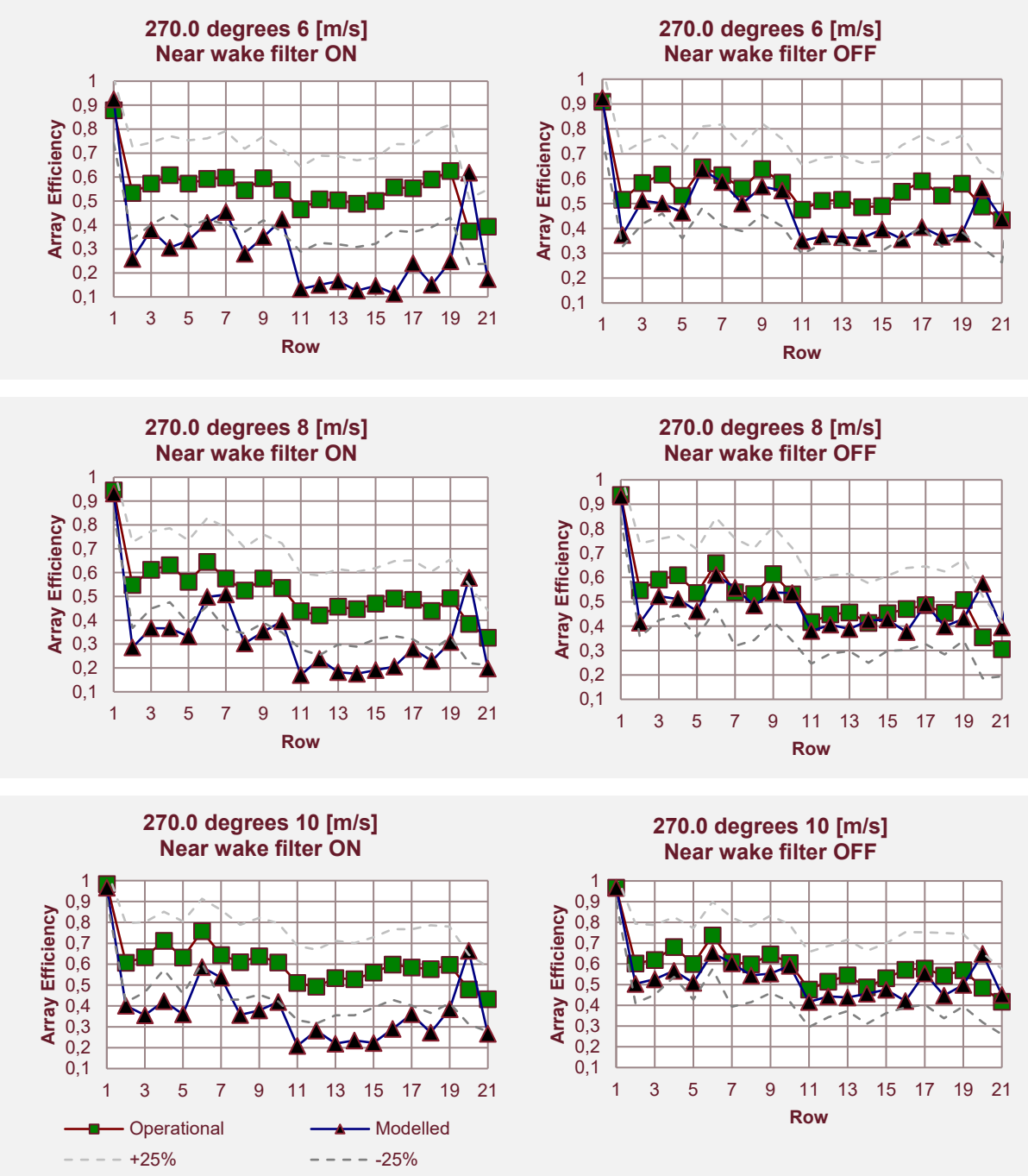

Figure 3: Effects of enabling and disabling the EV near wake filter – Example 2

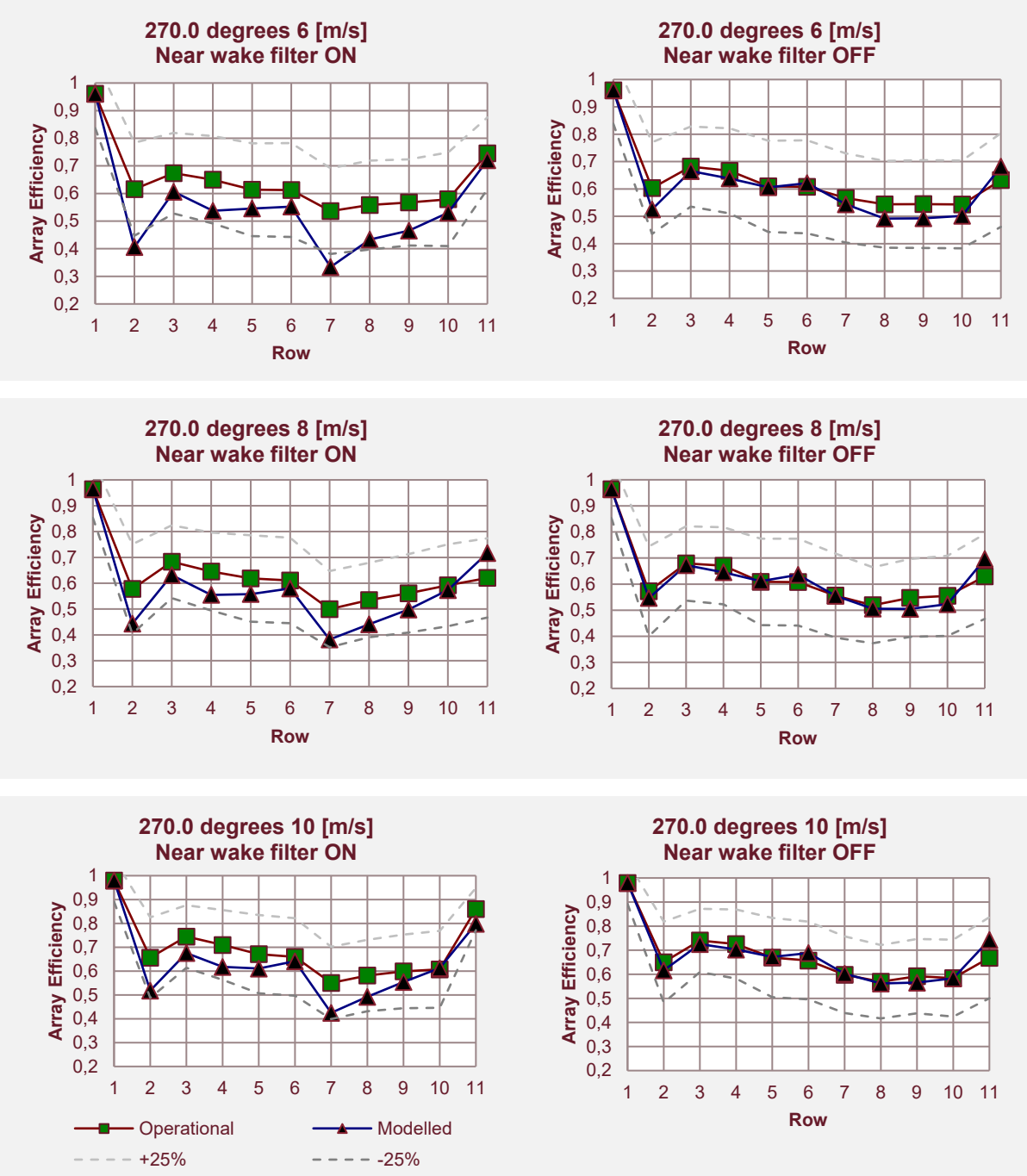

Figure 4: Effects of enabling and disabling the EV near wake filter – Example 3

7. Offshore Results

7.1 Offshore Test Sites

The following results include a diverse set of projects from Europe and Asia. With the exception of test site 4, they are not described in any detail in order to preserve the anonymity of the data.

7.1.1 Offshore Test Site 1

This offshore test site consists of around 90 larger (>5MW) turbines with several surrounding wind farms. However, any directions in which the project is waked by other projects are excluded. While this project is not a perfectly regular grid, there are some directions in which it can be considered up to 17 rows deep and other with as few as four to eight rows.

For this project, nearby meteorological mast data was unavailable so a Weather Research and Forecasting Model (WRF) was used to synthesize a virtual met mast.

The following chart shows the optimal turbine roughness length for this site appears to be 1.9m as this is when the overall mean wake error is close to zero. As turbine roughness decreases, it is observed that the magnitude of the mean wake error increases but the modeling error remains relatively flat for values of turbine roughness above 1.2m.

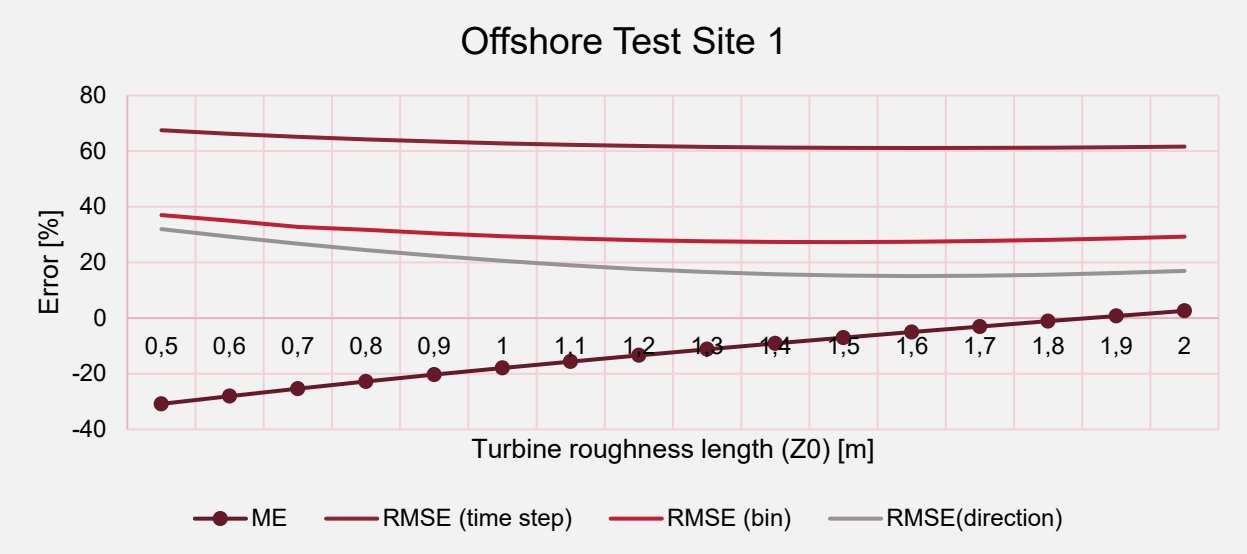

Figure 5: Offshore Site 1 variation in error metrics with turbine roughness

The following figure shows per bin modeled wake losses compared to operational wake losses.

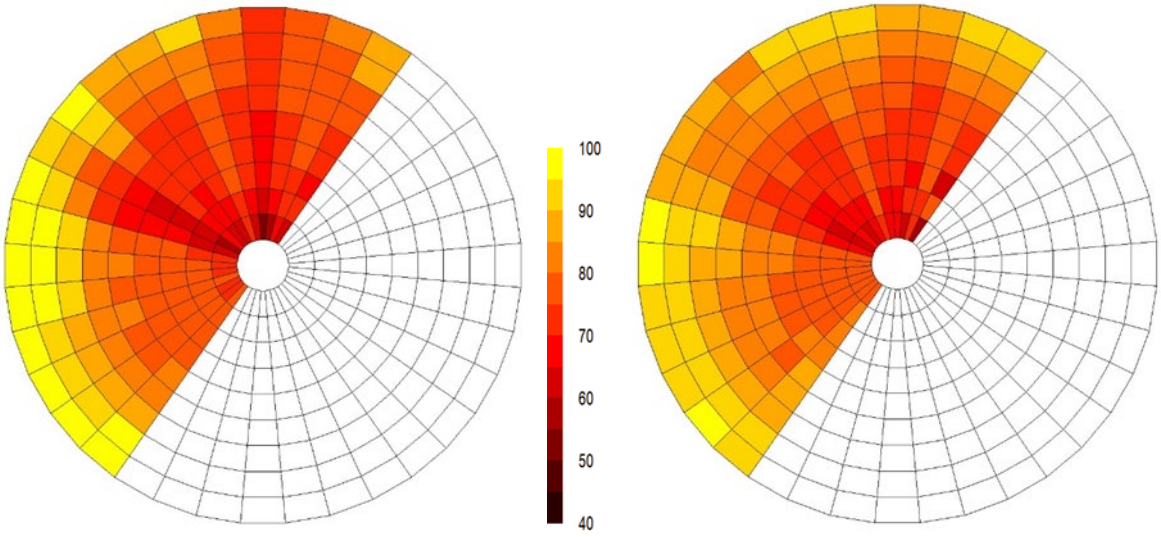

Figure 6: Offshore Site 1 overall wake mean array efficiency by speed and direction

Unless otherwise stated, for the remainder of these graphs in this report, the innermost rings represent the 5m/s bin, and the outermost rings represent the 13m/s bin. The white cells represent directions in which usable SCADA data was unavailable for the front row turbines.

7.1.2 Offshore Test Site 2

This site is a small, isolated wind farm consisting of approximately five rows of 5MW turbines in a wind regime, which has a distinctly uniform wind direction. While it is fairly close to the coast, the upwind fetch in the predominant direction is well over 100km.

For this project, a met mast located on the upwind side of the project and was used to model the freestream conditions (ignoring any global blockage effect).

The following chart shows the optimal turbine roughness length for this site appears to be 1.5m as this is when the overall mean wake error is close to zero. As turbine roughness decreases, it is observed that the magnitude of the mean wake error increases but the modeling error remains relatively flat for values of turbine roughness between 1.2m and 2m.

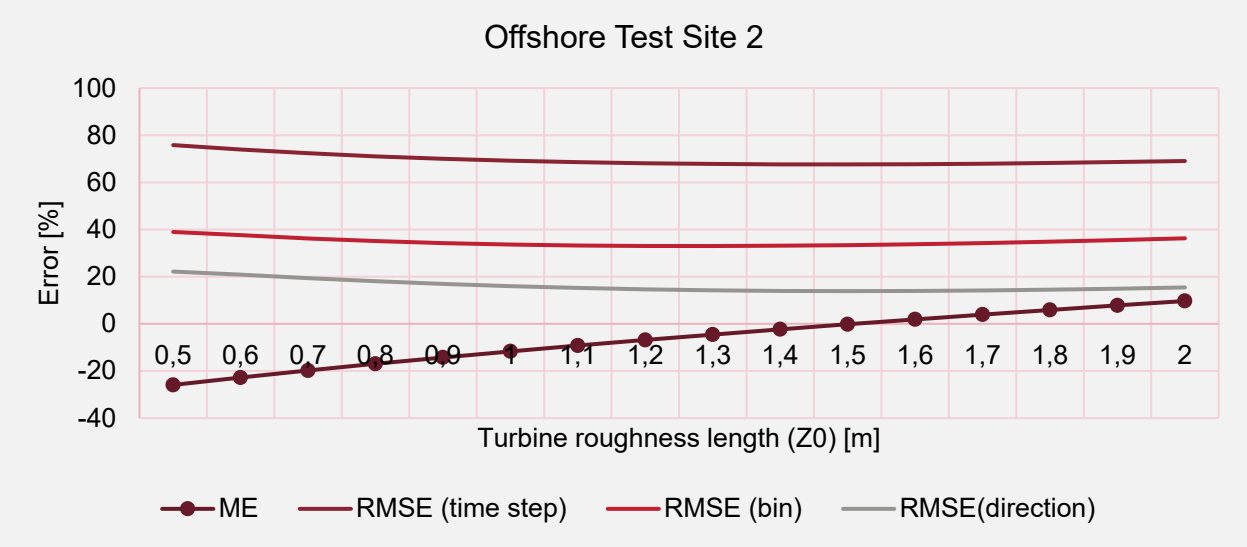

Figure 7: Offshore Site 2 variation in error metrics with turbine roughness

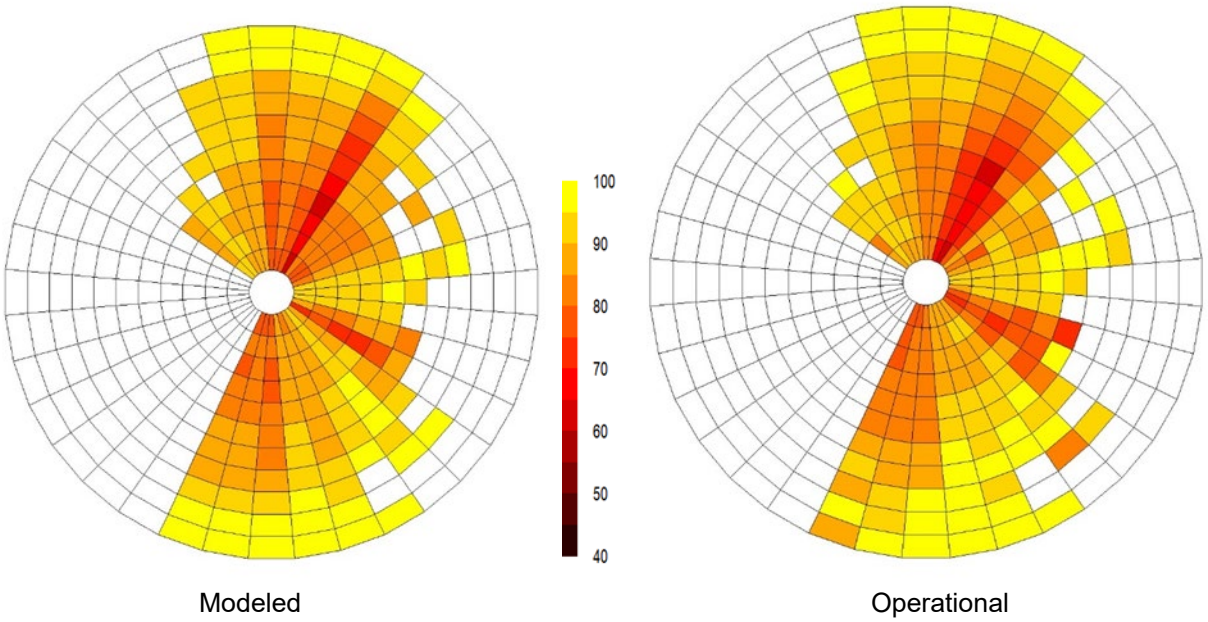

Figure 8: Offshore Site 2 overall wake mean array efficiency by speed and direction

7.1.3 Offshore Test Site 3

This is a gridded array of slightly older turbines. Nearby meteorological mast data was unavailable so a virtual met mast was created from a mix of SCADA wind speed and direction data, a WRF run and ERA5 data. The use of the virtual met mast leads somewhat predictably to higher modeling errors in this case. However, it still proves possible to extract wake behavior for a range of directions and tuning the modeled wake loss yields a turbine roughness of 1.5m.

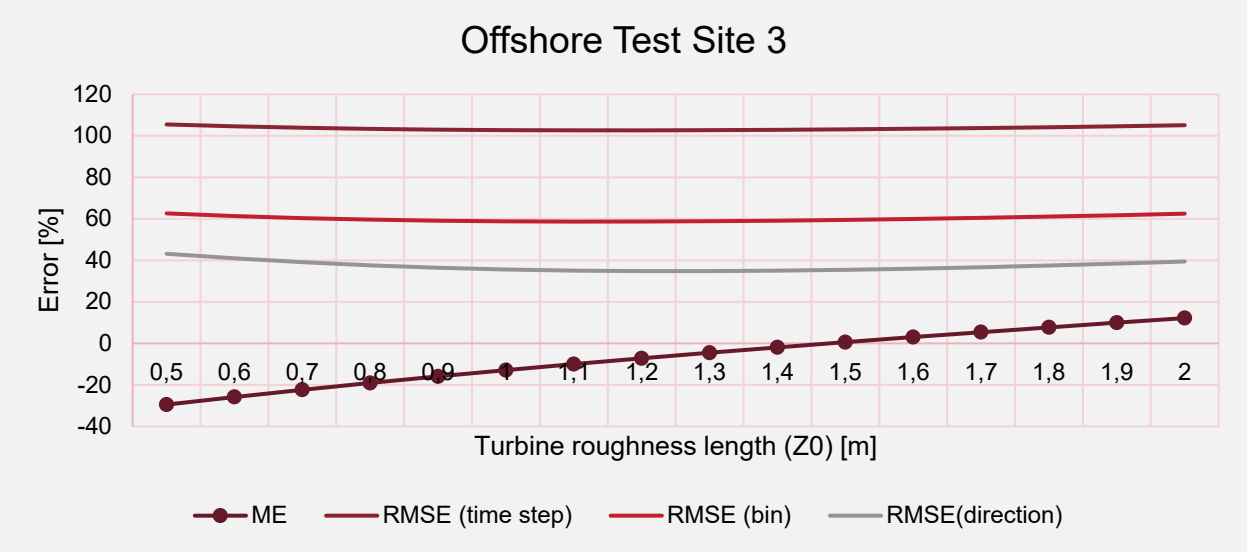

Figure 9: Offshore Site 3 variation in error metrics with turbine roughness

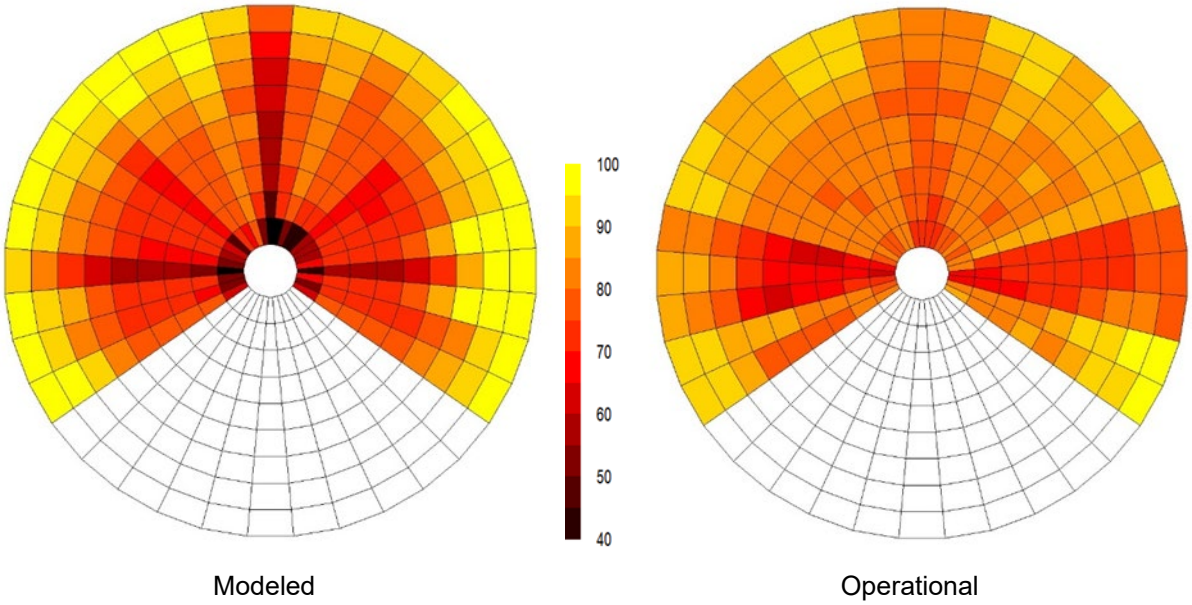

Figure 10: Offshore Site 3 overall wake mean array efficiency by speed and direction

In this case, while we see a low overall bias, the model does less well at predicting the pattern of wake losses with speed and direction.

7.1.4 Offshore Test Site 4 (Egmond An Zee)

For this project, Shell allowed UL Solutions to use SCADA production data from their Egmond An Zee wind farm in the North Sea. Egmond An Zee is a somewhat older farm consisting of 36 Vestas 2MW turbines arranged in a gridded formation, four rows deep relative to the predominant wind direction which is from the Southwest. There is a met mast just in front of the front row and this has been used as the basis for the freestream conditions. Due to the commissioning of the Princess Amalia wind farm less than 9km upwind, only the first 18 months of operational data have been used in this study.

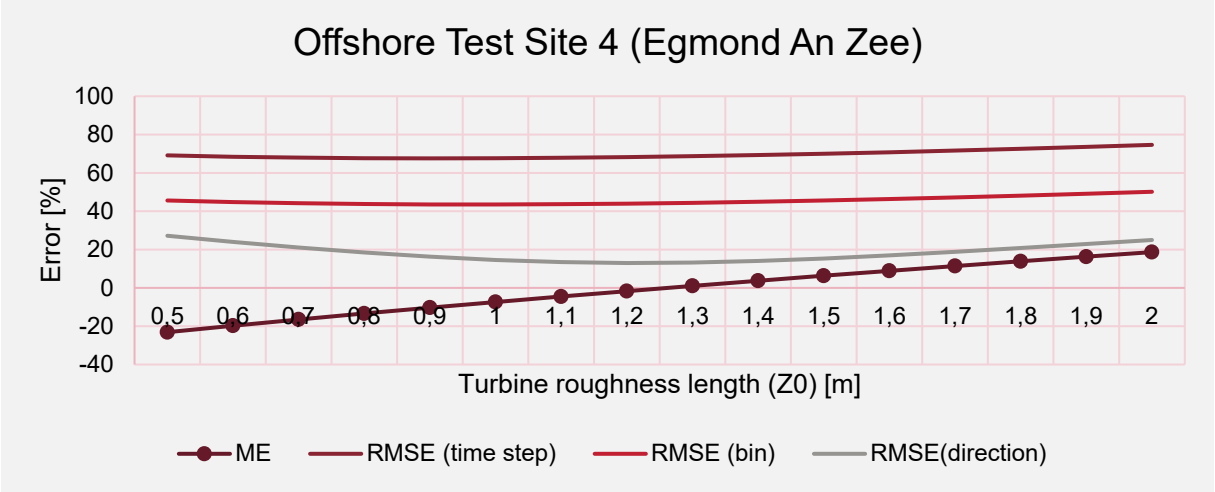

Figure 11: Offshore Site 4 variation in error metrics with turbine roughness

Egmond An Zee points to an optimal turbine roughness of 1.3 which is broadly in line with sites 2 and 3.

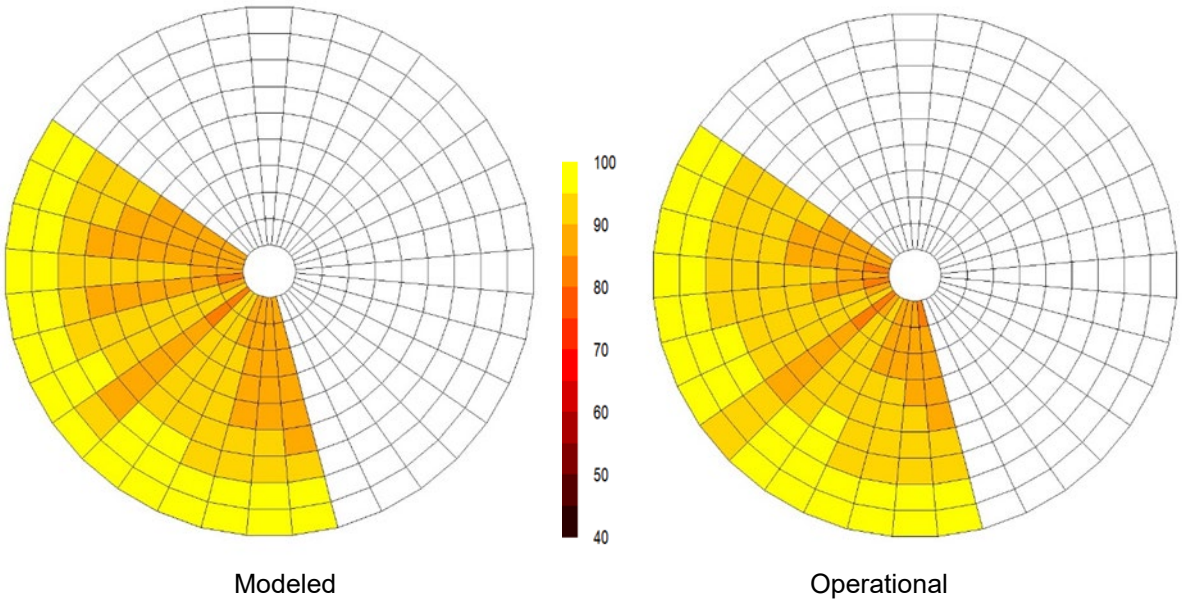

Figure 12: Offshore Site 5 overall wake mean array efficiency by speed and direction

7.1.5 Offshore Test Site 5

The fifth wind farm consists of over 100 turbines, which form a dispersed array with up to eight rows in one direction and up to 20 rows in other directions. A nearby met mast which can be used to provide freestream conditions was used in this case to drive the wake analysis.

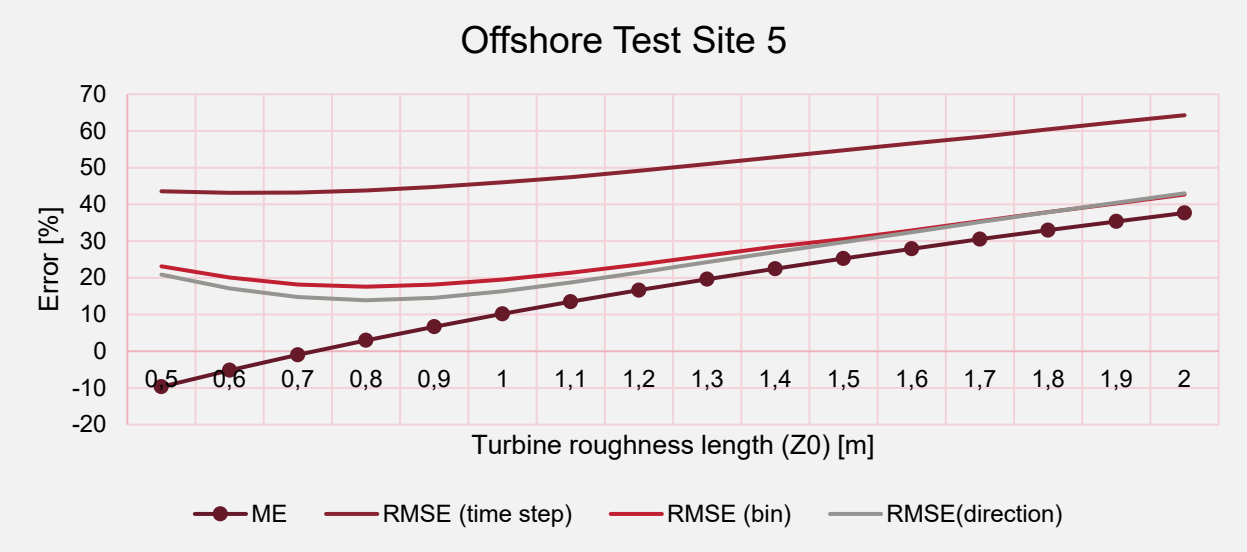

Figure 13: Offshore Site 5 variation in error metrics with turbine roughness

Running the wake analysis at every 0.1m of turbine roughness length between 0.5 and 2m indicates an optimal value of between 0.7 and 0.75m. Again, this seems like a surprisingly low value but is supported by a minimum in RMSE between 0.7 and 0.9m.

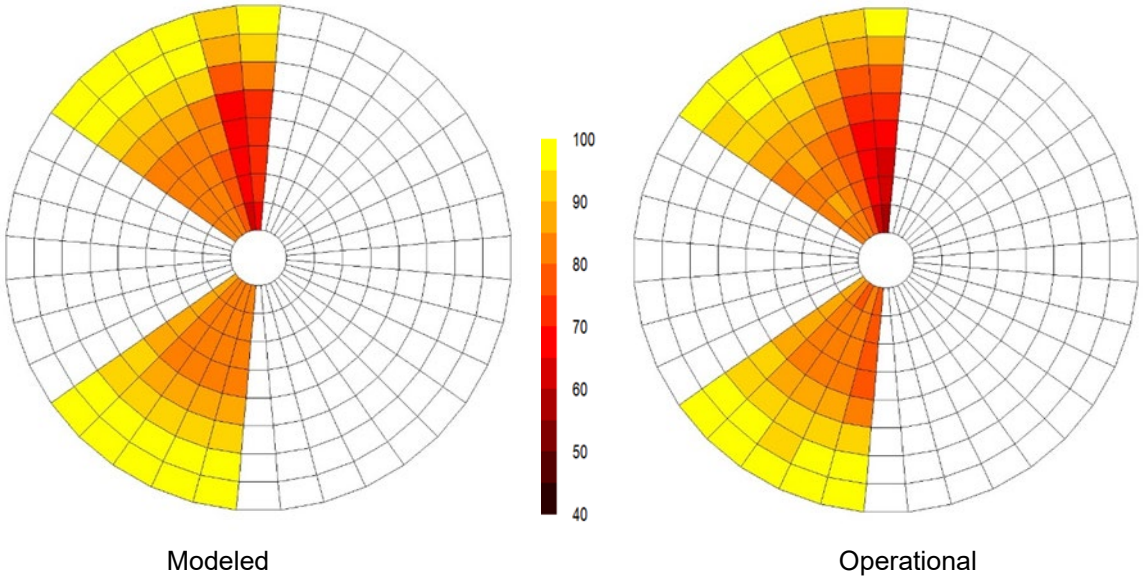

Figure 14: Offshore Site 5 overall wake mean array efficiency by speed and direction

7.2 Orsted offshore wake bench

In addition to UL Solutions own in-depth analysis of the five sites above, results were also submitted to the Orsted wake bench (Nygaard et al. 2022, and Johansson, E., Wind Europe 2023). The Orsted wake bench modeling validation assumes reference freestream locations that minimize global blockage impacts, and consequently demonstrates that the implicit modeling of global blockage through DAWM and RHB settings does a reasonable job of characterizing total array losses in an unbiased way.

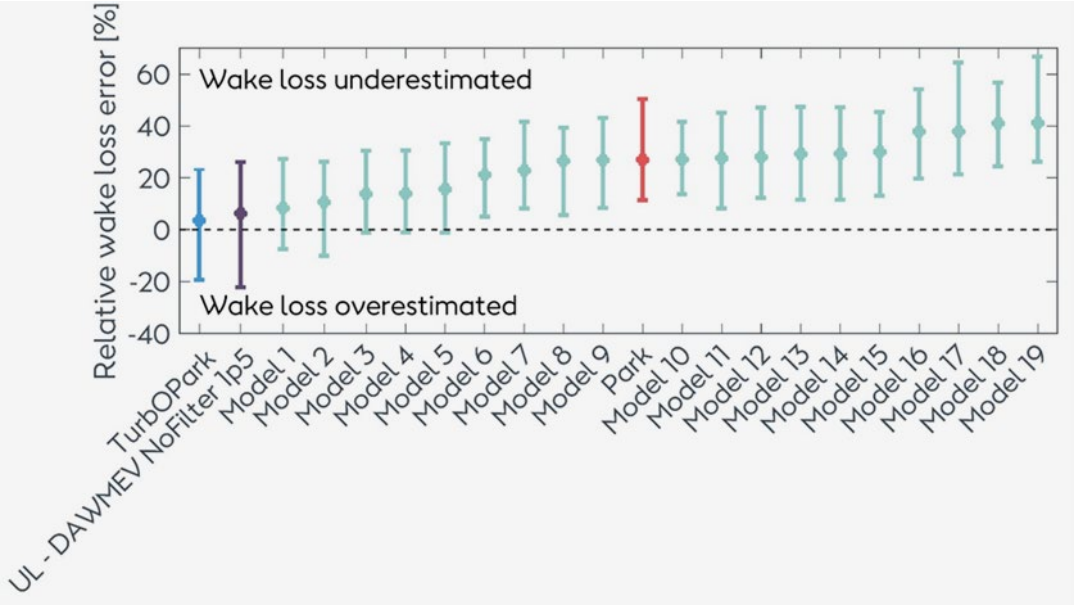

Figure 15: Orsted wake validation results

Comparing mean bias across all projects for a variety of industry models and implementations. The second model from the left uses a turbine roughness length of 1.5m and removes the near wake filter from the Eddy Viscosity portion of the DAWM EV wake model.

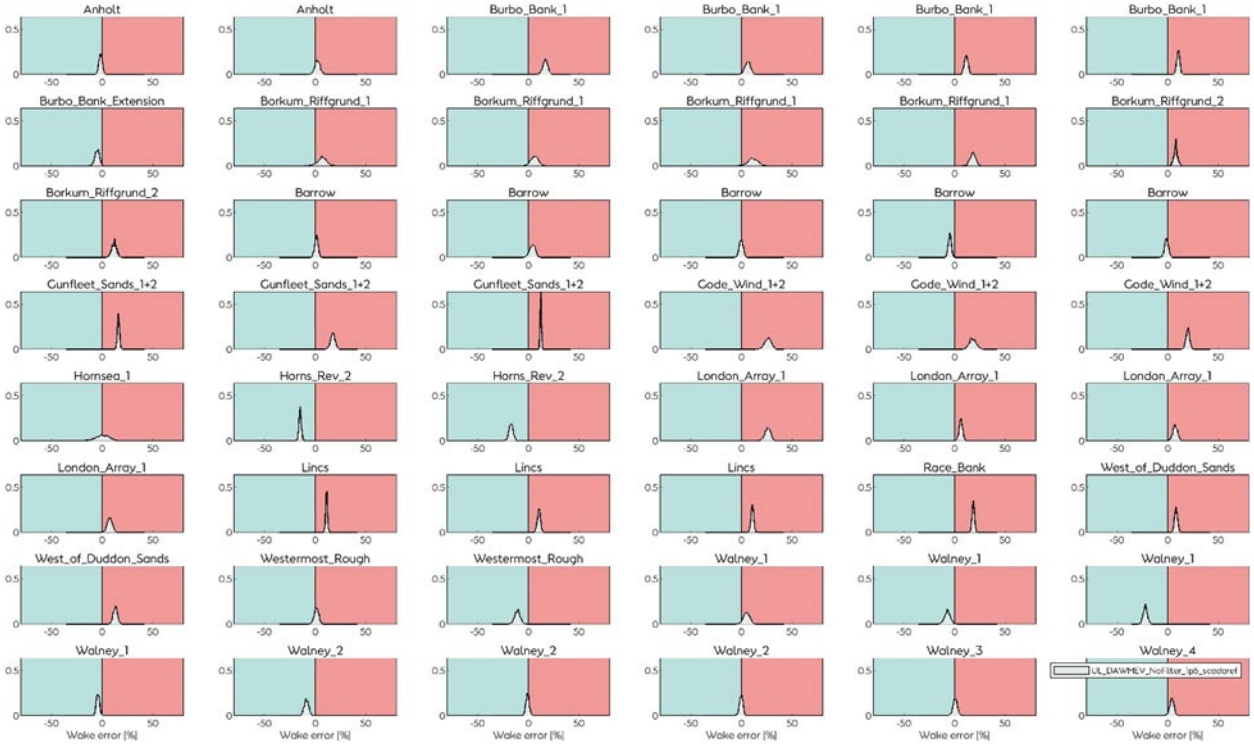

Figure 16: Orsted bootstrapped error distributions per wind farm for DAWM EV with a turbine roughness length of 1.5m and no near wake filter

.

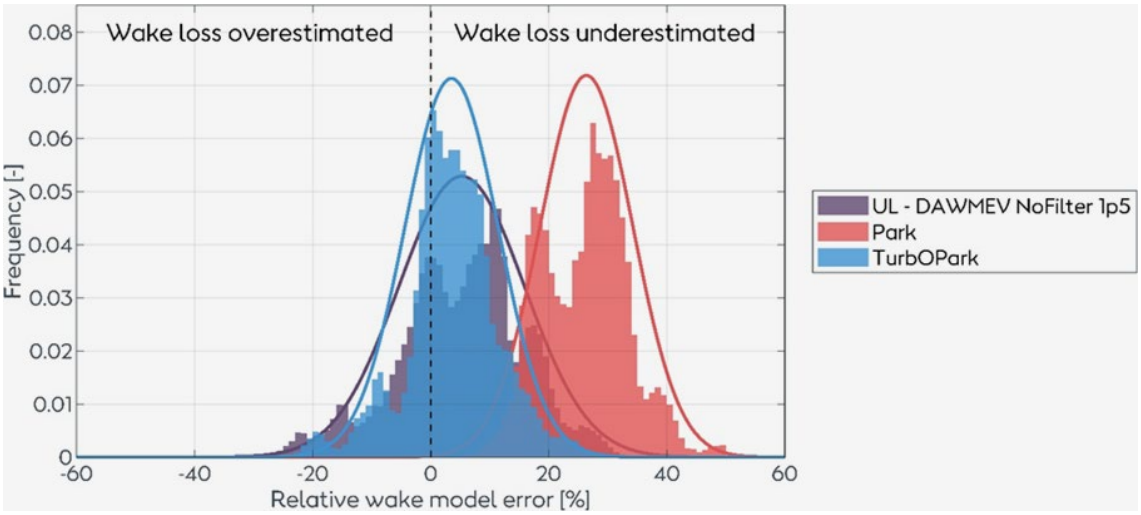

Figure 17: Orsted Error distribution across all wind farms Park, TurbOPark and the DAWM EV with a turbine roughness of 1.5m and near wake filter off

7.3 Offshore conclusions

The large spread of mean biases across the five sites combined with the fact that none of the results presented here include any explicit modeling of any global blockage effect encourages a slightly conservative approach. Combined with the Orsted wake bench results, UL Solutions is now recommending a turbine roughness of 1.5m for modeling offshore wind farms.

Combining results from the five projects described above, bootstrapping can be used to synthesize a population of errors for each project. The bootstrapped results shown below are for 1,000 random samples with replacement, repeated 10,000 times. Ideally, these populations substantially overlap and can then be combined to give a single mean error and standard deviation. However, for the five sites analyzed here, the overall mean biases are too far apart to give a coherent error population as can be seen from Figure 15 below.

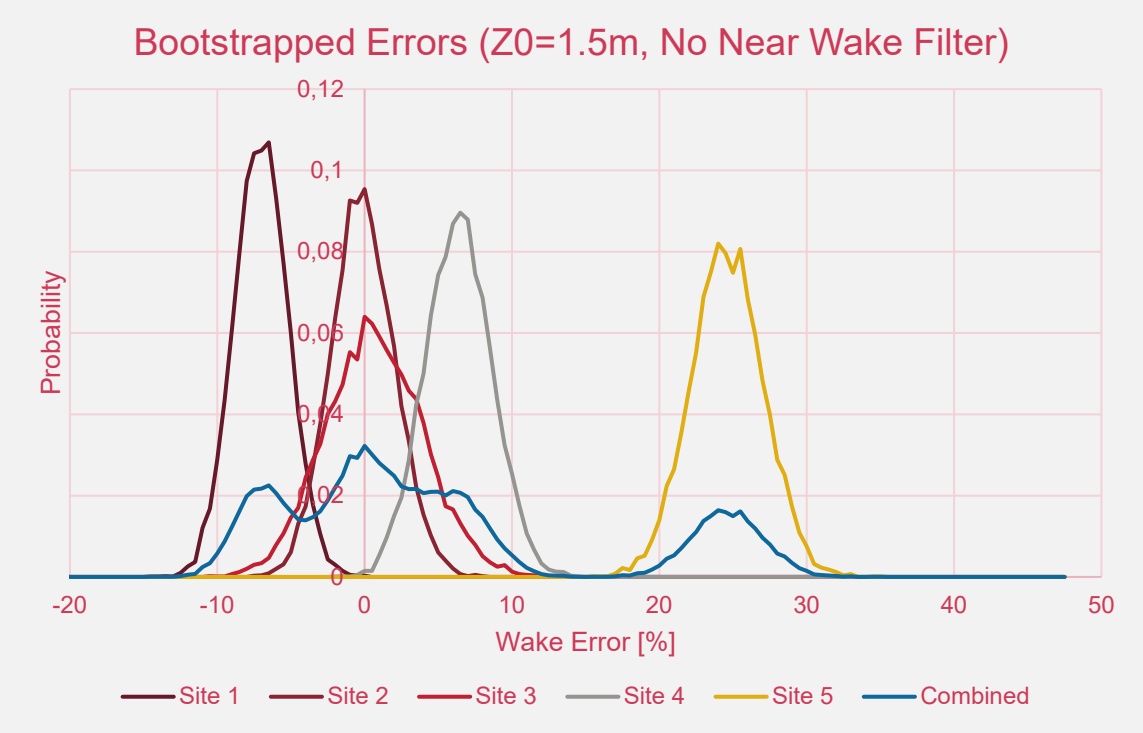

Figure 18: Bootstrapped errors for each offshore test site plus the combined errors across all five offshore sites

The mean and standard deviation of the errors shown in Figure 15 are 4.9% and 11% respectively. This points to an array loss uncertainty standard deviation of somewhere between 12% and 16%. However, this is complicated somewhat by the presence of an overall bias together with the fact that the errors are so different amongst the different projects. It is important to stress here that all these error percentages are calculated relative to the inferred array loss and not as a fraction of the overall energy yield.

A limitation on the work reporting herein is the lack of true freestream measurements or sufficient information to be able to remove turbine underperformance beyond simply adjusting the front row power output to that predicted by the power curve. For these reasons, we were not able to confirm, deny nor quantify any global blockage effect. We have applied a simple RHB induction model to sites 1 to 5 as well as to the results submitted to the Orsted wake bench.

From a qualitative point of view, Offshore Sites 2 and 3 show zero mean bias, Offshore Site 1 shows a negative mean bias, Offshore Sites 4 and 5 show a positive mean bias. The Orsted wake bench shows a slight under-estimate of wake losses for this DAWM EV configuration. UL Solutions is also choosing to dispense with the Eddy Viscosity near wake filter in this update as we have multiple onshore observations, which show that it leads to too strong wake effects for turbines that are close together and directly inline. Abandoning the near wake filter leads to a decrease in overall wake losses and so necessitates an increase in the deep array effect to compensate.

These observations, coupled with the fact we are not explicitly modeling a global blockage effect, encourage UL Solutions to adopt a somewhat conservative approach using a turbine roughness length of 1.5m coupled with the RHB induction model. UL Solutions considers this a reasonable and relatively unbiased approximation of total array effects and assumes an equivalent annual energy prediction uncertainty of 20%.

8. Onshore Results

Identities and locations of the onshore sites are confidential to preserve anonymity though site descriptions are provided to aid in interpretation of results.

8.1 Onshore Test Sites

8.1.1 Onshore Test Site 1

This is an older site arranged in five rows with inter-row spacing of around 18 RDs and intra-row spacing of around 4 RDs. The project is sited in mixed farmland with an estimated background roughness length around 0.07m and is relatively flat. It has met masts on either end of the site, which means we can assemble un-waked results for all wind directions.

The near wake filter in the EV model results in very clearly over-predicted wakes when the wind is blowing along the four RD-separated rows of turbines. Switching off the near wake filter and tuning for an overall mean bias close to zero gives a turbine roughness of 2.2m, when used in conjunction with the RHB induction model.

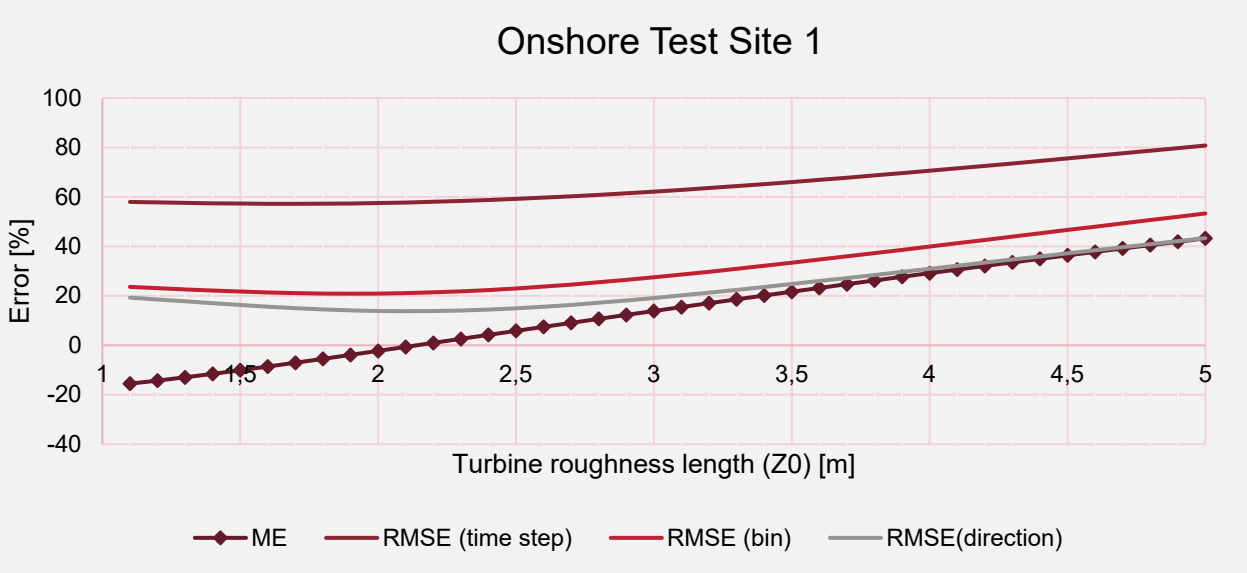

Figure 19: Onshore Site 1 variation in error metrics with turbine roughness length

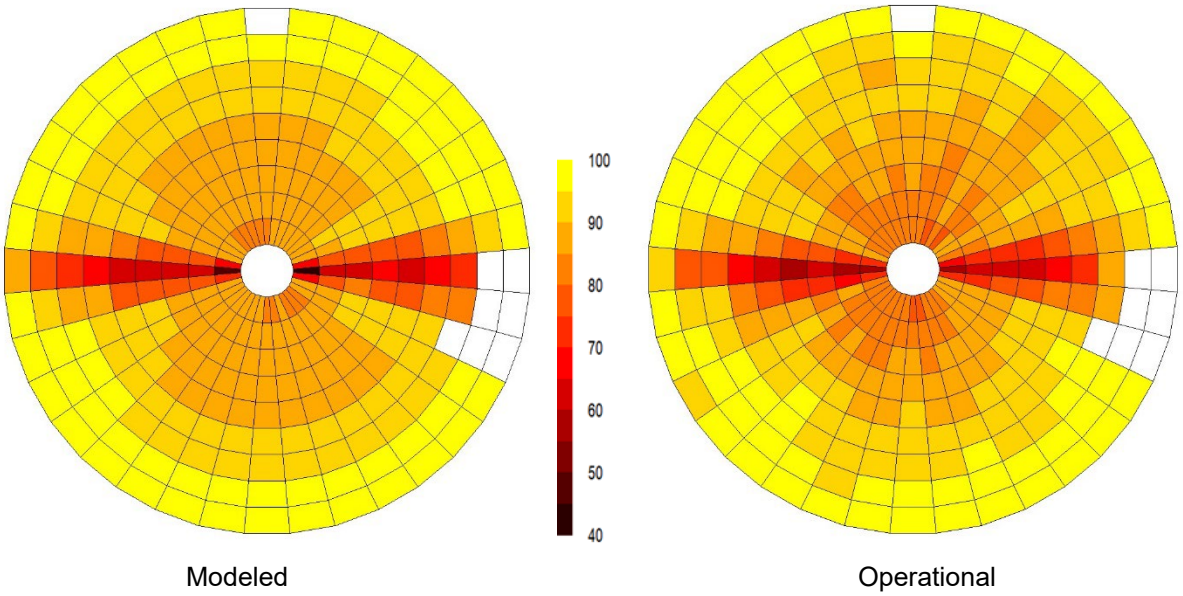

Figure 20: Onshore Site 1 mean array efficiency by speed and direction

The distribution of array efficiencies with wind speed and direction show that while the operational data is less smooth, the overall pattern is well captured by the model. The data used in this analysis represents around 45% of the total energy production and a zero ME is given by a turbine roughness length of 2.2m.

8.1.2 Onshore Test Site 2

This is a slightly older, 70-turbine site with other wind farms on either side of it. Overall, there are in excess of three hundred turbines in fairly close proximity to this layout. The turbines of this site are again oriented in rows, with an interrow spacing of around 15 RDs and an intra-row spacing of around 3 RDs. Two different met masts were used in order to assemble sufficient un-waked directions. The terrain is very gently sloping with a background roughness of around 0.07m.

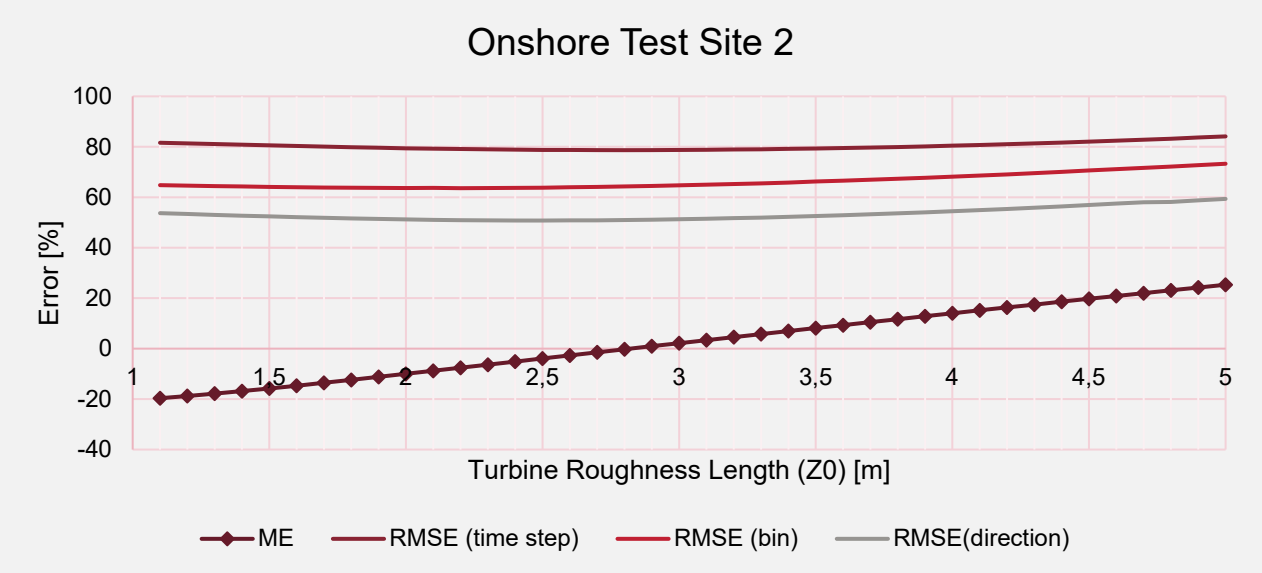

Figure 21: Onshore Site 2 variation in error metrics with turbine roughness

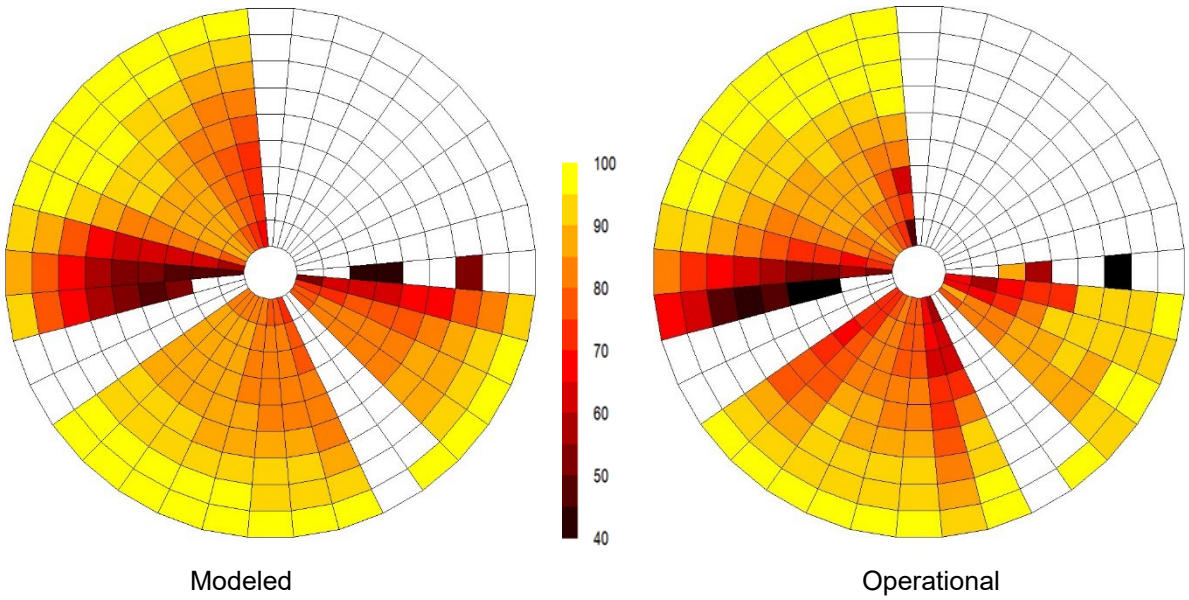

Figure 22: Onshore Site 2 mean array efficiency by speed and direction

The data used in this analysis represents around 45% of the total energy production and a zero ME is given by a turbine roughness length of 2.8m.

8.1.3 Onshore Test Site 3

Onshore Test Site 3 is a relatively small, isolated site of around thirty turbines on a small raised flat area with terrain dropping off steeply on three sides. Background roughness is estimated to be around 0.07m. The turbines are oriented in rows perpendicular to the dominant wind directions with a spacing of around 9 RDs by 3 RDs.

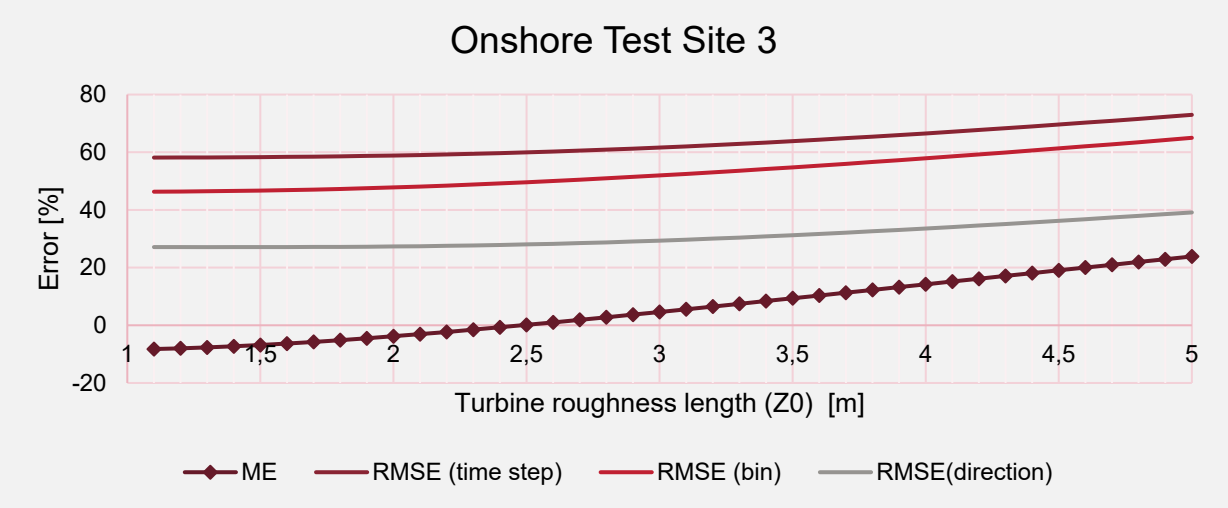

Figure 23: Onshore Site 3 variation in error metrics with turbine roughness

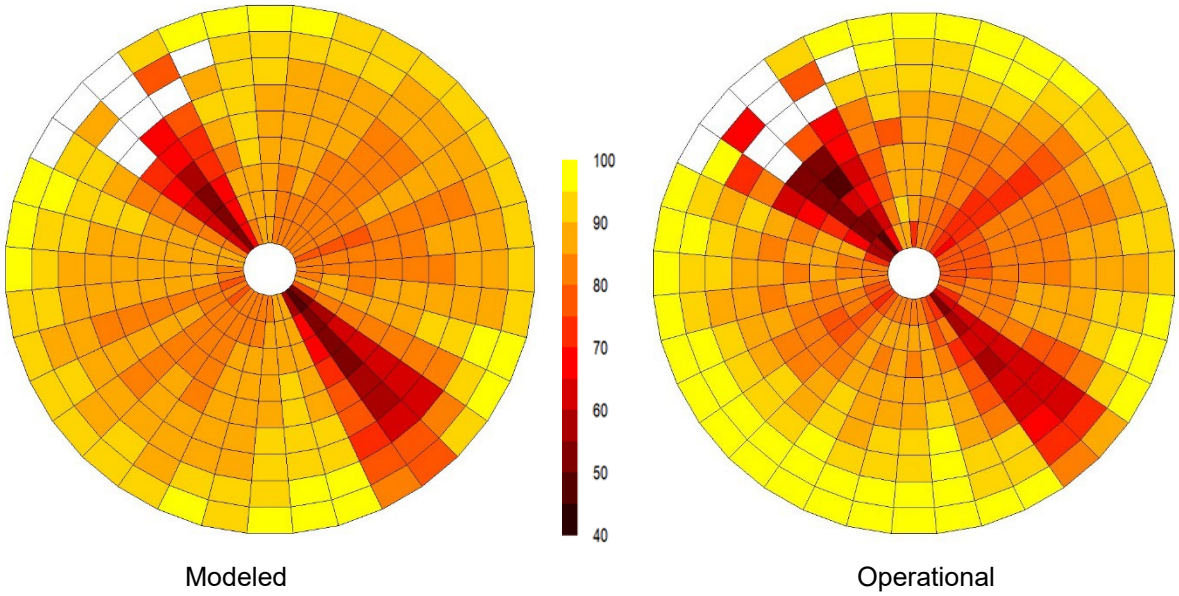

Figure 24: Onshore Site 3 mean array efficiency by speed and direction

The data used in this analysis represents around 43% of the total energy production and a zero ME is given by a turbine roughness length of 2.5m.

8.1.4 Onshore Test Site 4

Onshore Test Site 4 is a large project with over one hundred turbines and a small neighboring wind farm to one side. The project is organized into several rows oriented perpendicular to the dominant wind directions with approximate spacing of 20 RDs by 2 RDs. The project is situated on a slight rise above terrain which is otherwise mostly flat with an estimated background roughness around 0.05m.

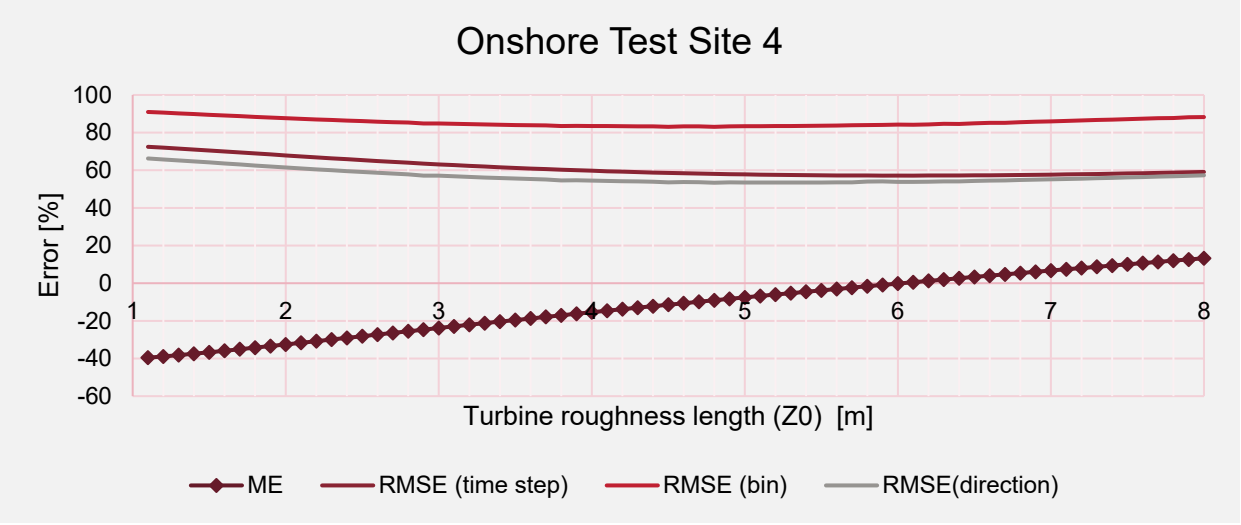

Figure 25: Onshore Site 4 variation in error metrics with turbine roughness

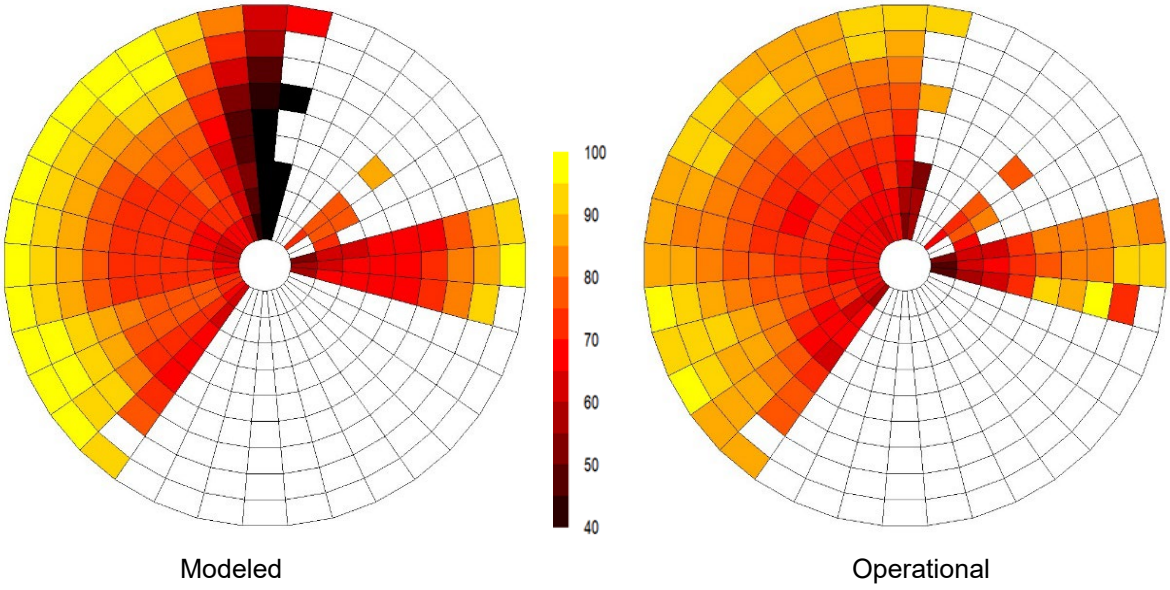

Figure 26: Onshore Site 4 mean array efficiency by speed and direction

The data used in this analysis represents around 22.5% of the total energy production and a zero ME is given by a turbine roughness length of 6.0m. As can be seen from Figures 22 and 23, the modeling error for this project is quite high and even the overall error by wind speed and direction bin stays stubbornly high throughout the range of potential values of turbine roughness.

8.1.5 Onshore Test Site 5

Onshore Test Site 5 consists of around 70 turbines with another 200 turbines to either side but fortunately nothing directly upwind in the dominant direction. The estimated surface roughness is approximately 0.05m.

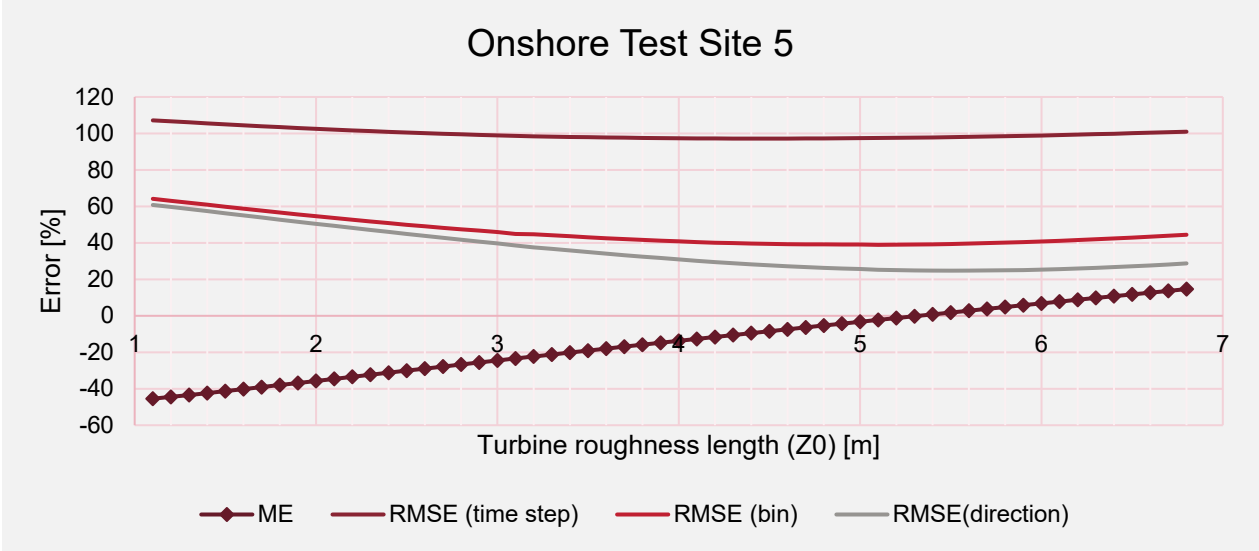

Figure 27: Onshore Site 5 variation in error metrics with turbine roughness

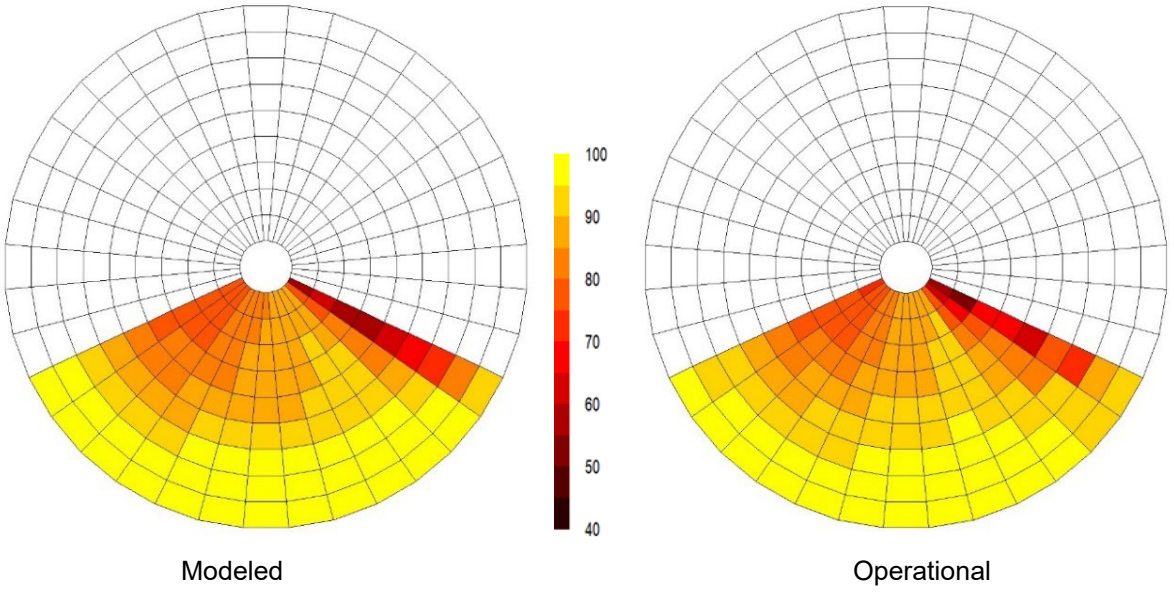

Figure 28: Onshore Site 5 mean array efficiency by speed and direction

The data used in this analysis represents around 33% of the total energy production and a zero ME is given by a turbine roughness length of 5.3m.

8.1.6 Onshore Test Site 6

Onshore Test Site 6 represents a valley gap project with mountains on either side and the wind coming down the valley. The estimated surface roughness is approximately 0.07m to 0.10m. There are a number of different turbine types making up the project and many rows oriented perpendicular to the dominant wind direction. Turbine spacing varies between 13 and 15 RDs by 2.5 to 3 RDs.

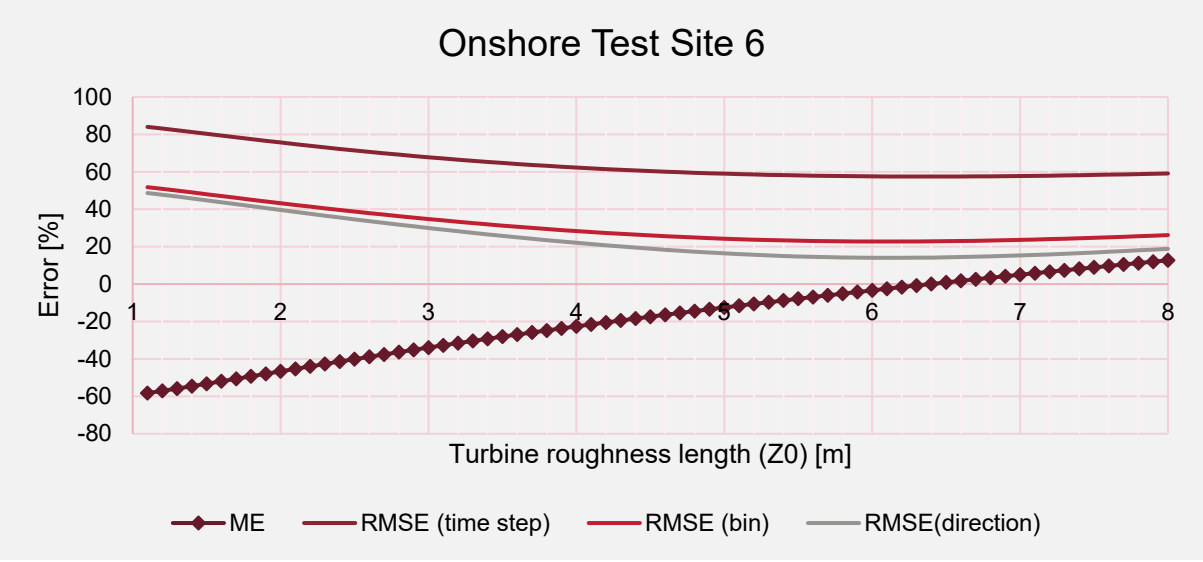

Figure 29: Onshore Site 6 variation in error metrics with turbine roughness

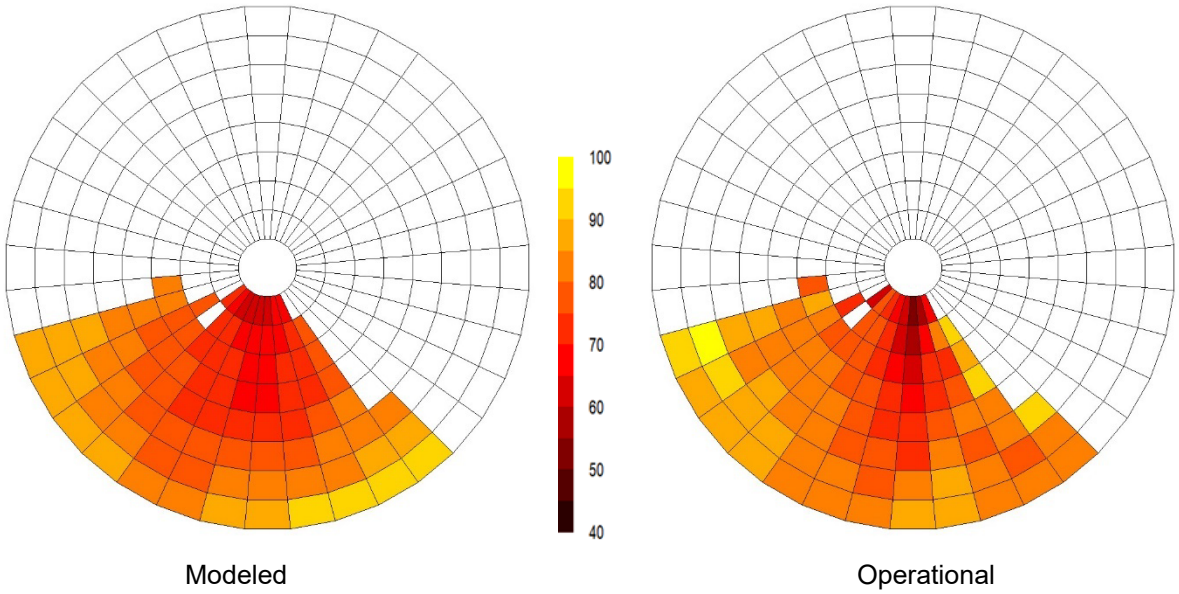

Figure 30: Onshore Site 6 mean array efficiency by speed and direction

The data used in this analysis represents around 25% of the total energy production and a zero ME is given by a turbine roughness length of 6.4m. This analysis was somewhat confounded by a variety of different turbines with different performance issues and retrofits over the years. However, the high turbine roughness required to model the wakes at this site is in line with expectations given the topography and wind regime.

8.1.7 Onshore Test Site 7

Onshore Test Site 7 is in very gentle terrain with an estimated roughness length of around 0.075m. Approximately 50 turbines are organized into several rows at an angle to the prevailing wind direction. Several other wind farms are downwind of this site and the met mast used in this study and thus, with the exception of any large-scale blockage effect, do not factor into this analysis.

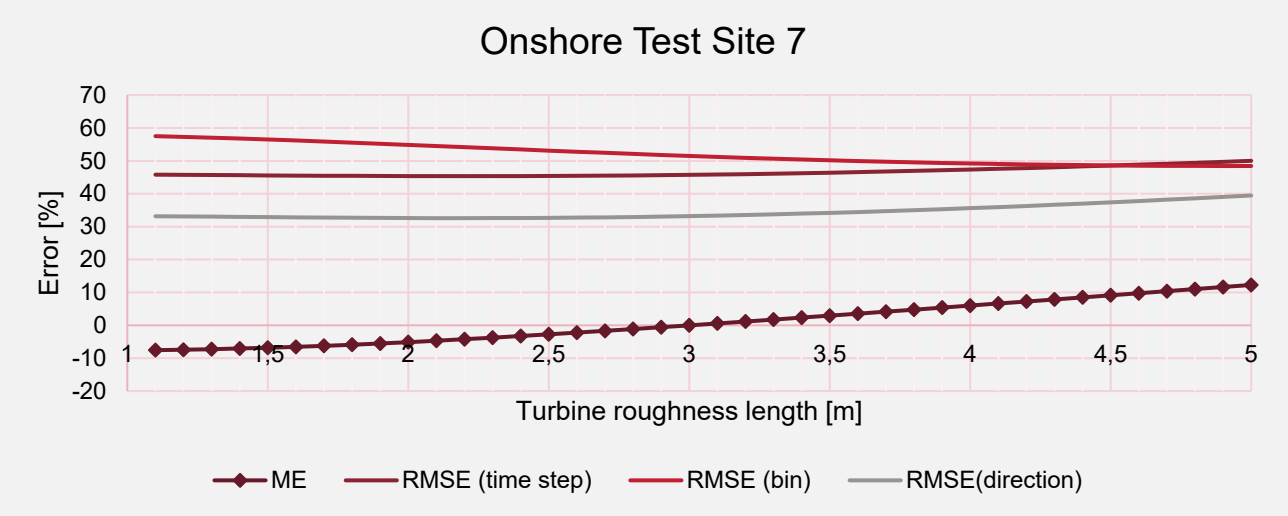

Figure 31: Onshore Site 7 variation in error metrics with turbine roughness

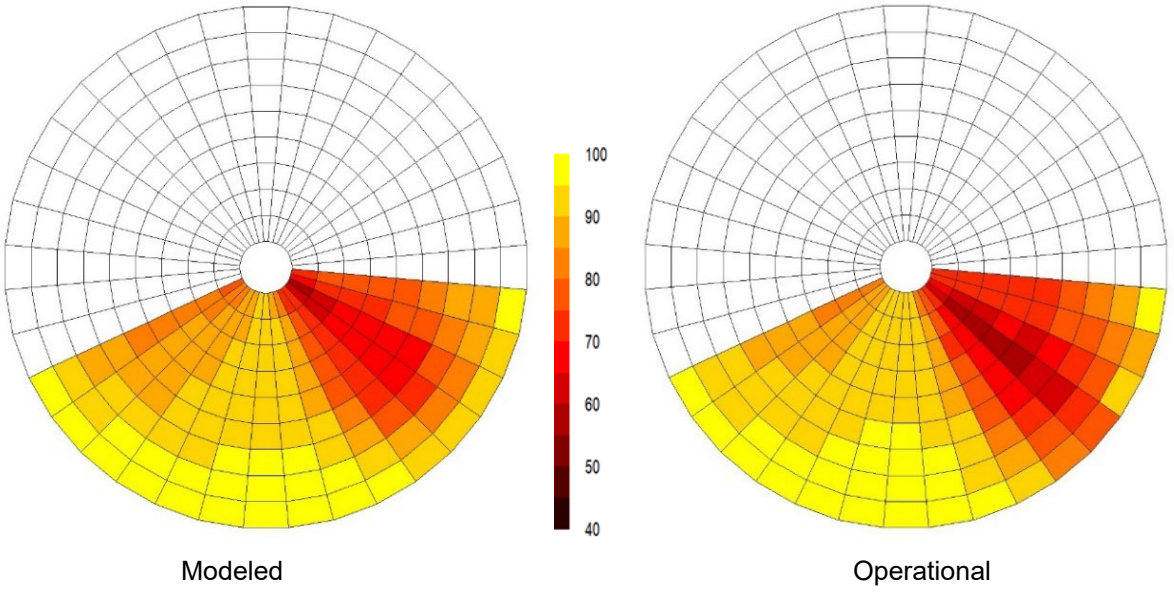

Figure 32: Onshore Site 7 mean array efficiency by speed and direction

The data used in this analysis represents around 45% of the total energy production and a zero ME is given by a turbine roughness length of 3.0m.

8.1.8 Onshore Test Site 8

Onshore Test Site 8 is sandwiched between other sites but does have some directions, which are un-waked at the met mast. The site is judged to have relatively low roughness at 0.03m and is also fairly flat with the wind turbines sitting at the edge of a very gently raised area, which sits around 50m above the surrounding area but with extremely shallow gradients.

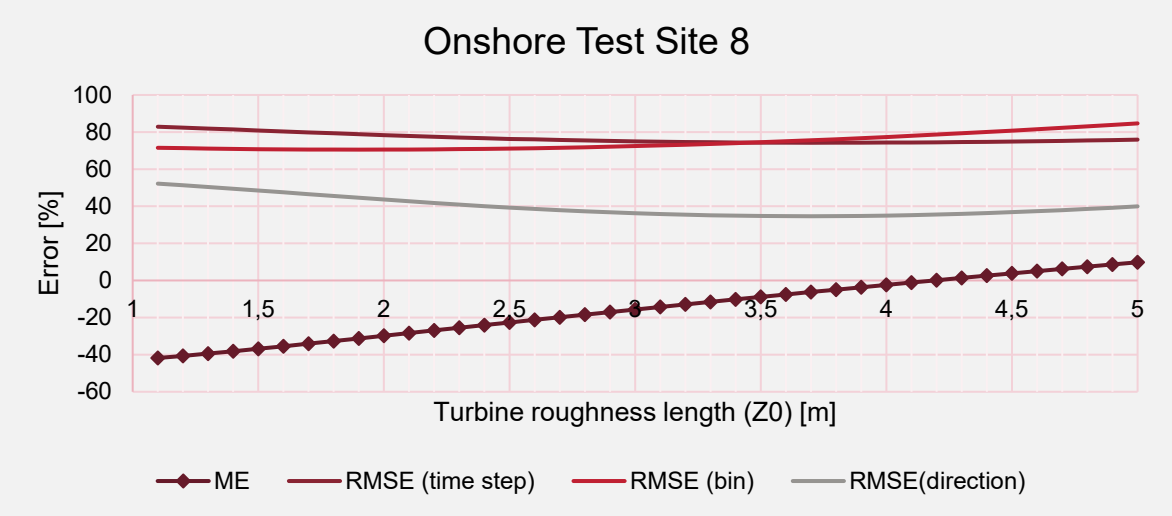

Figure 33: Onshore Site 8 variation in error metrics with turbine roughness

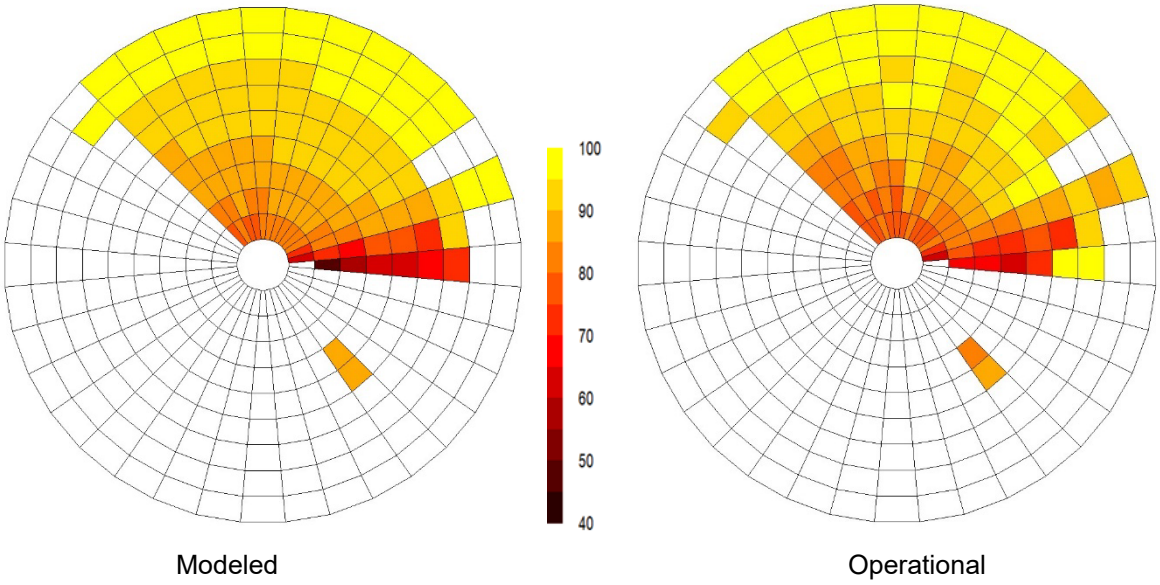

Figure 34: Onshore Site 8 mean array efficiency by speed and direction

The data used in this analysis represents around 15% of the total energy production and a zero ME is given by a turbine roughness length of 4.2m.

8.1.9 Onshore Test Site 9

Onshore Test Site 9 is around 70km away from the nearest other wind farms. It consists of nearly 40 turbines on a moderate ridge with an estimated surface roughness of 0.03m to 0.05m.

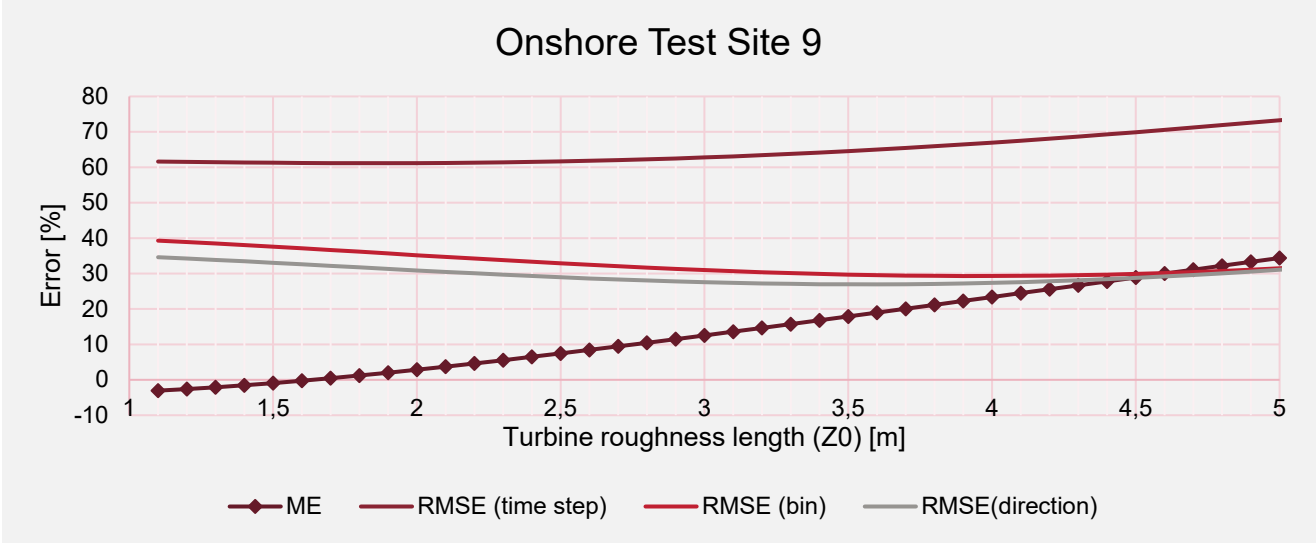

Figure 35: Onshore Site 9 variation in error metrics with turbine roughness

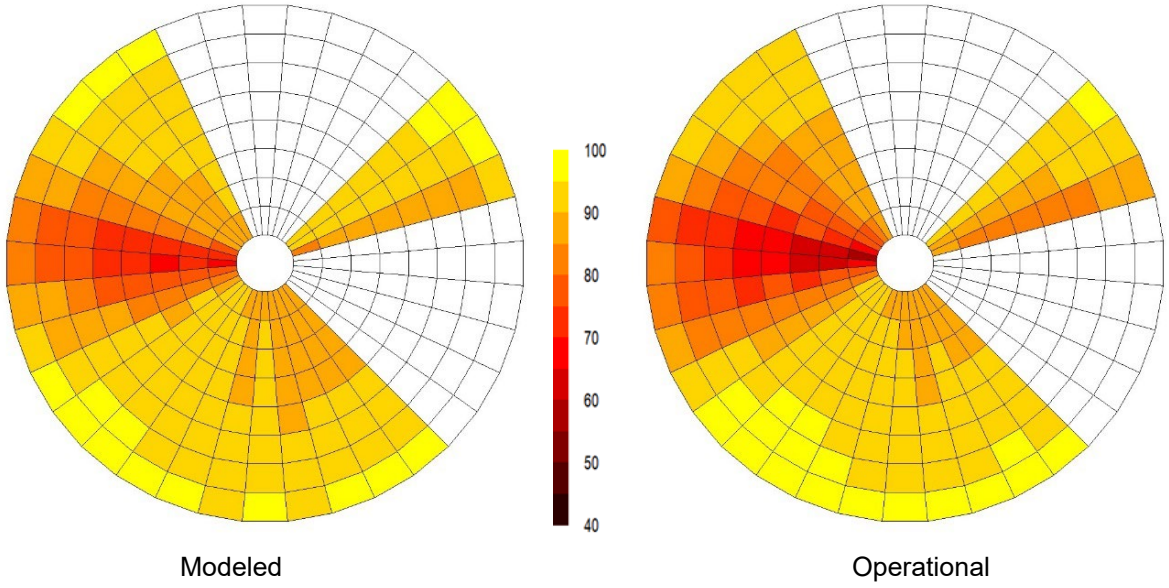

Figure 36: Onshore Site 9 mean array efficiency by speed and direction

In this case, the innermost rings still represent the 5m/s bin, while the outermost rings represent the 12m/s bin.

The data used in this analysis represents around 37.5% of the total energy production and a zero ME is given by a turbine roughness length of 1.7m.

8.1.10 Onshore Test Site 10

Onshore Test Site 10 has around 60 turbines in a large, flat valley bottom with an estimated surface roughness of 0.05m.

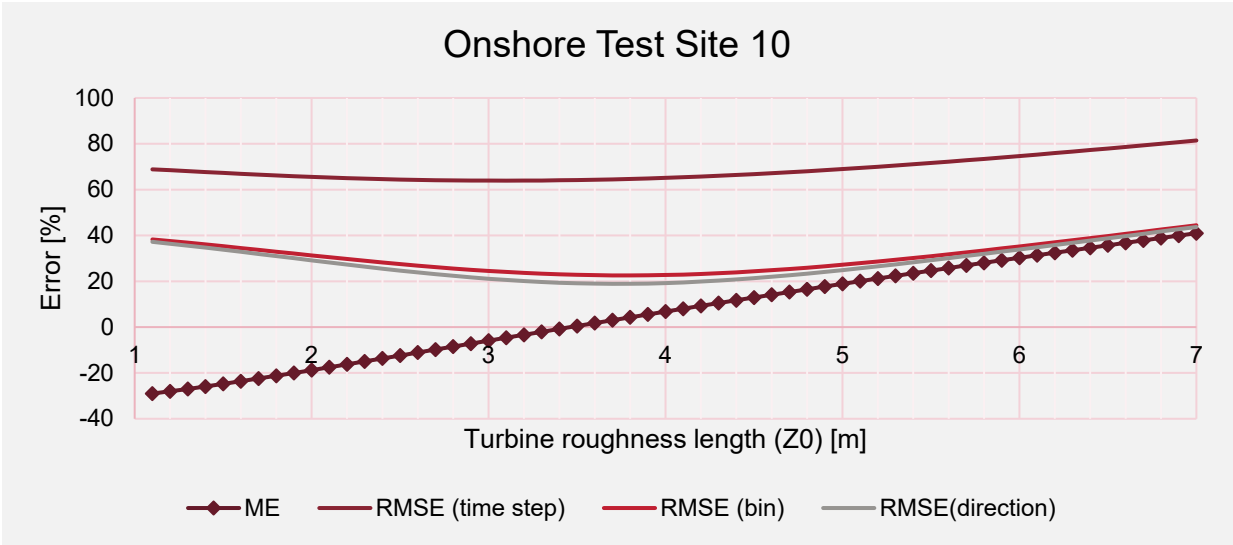

Figure 37: Onshore Site 10 variation in error metrics with turbine roughness

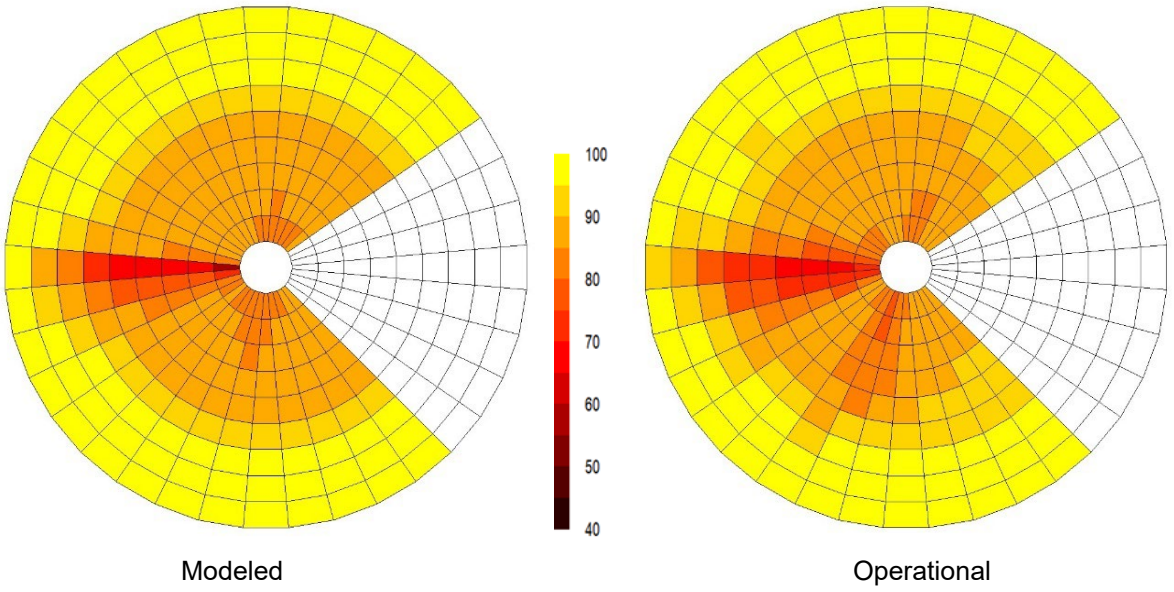

Figure 38: Onshore Site 10 mean array efficiency by speed and direction

The data used in this analysis represents around 63% of the total energy production and a zero ME is given by a turbine roughness length of 3.5m.

8.1.11 Onshore Test Site 11

Onshore Test Site 11 is a larger wind farm with around 100 turbines with two other wind farms between 15 and 30km away. The site has a background roughness between 0.07 and 0.5 and is almost flat, with very gentle gradients in every direction.

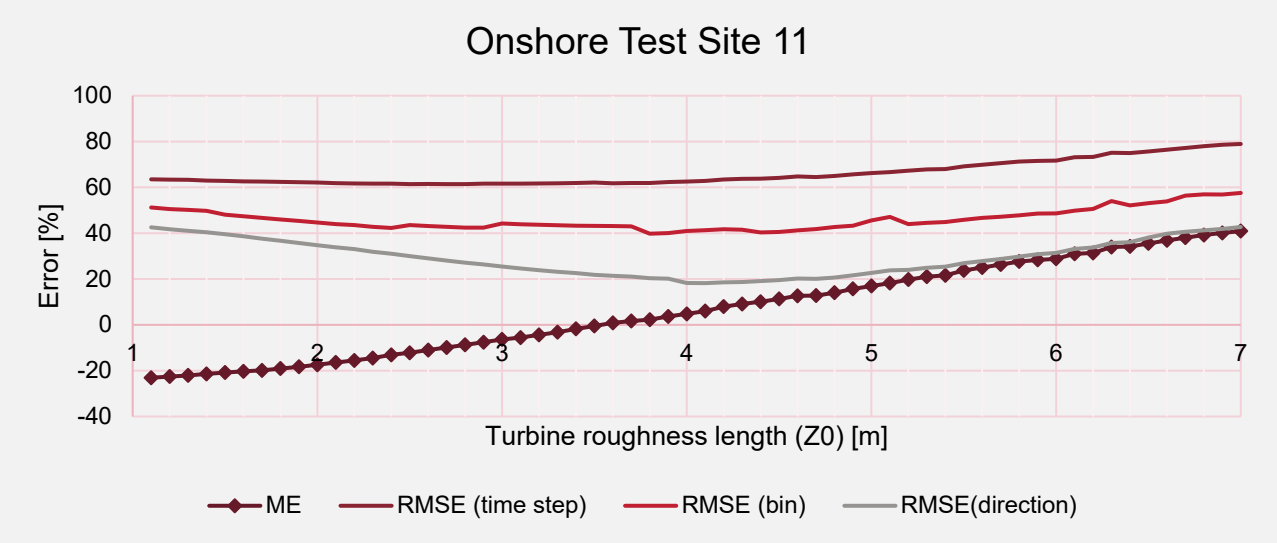

Figure 39: Onshore Site 11 variation in error metrics with turbine roughness

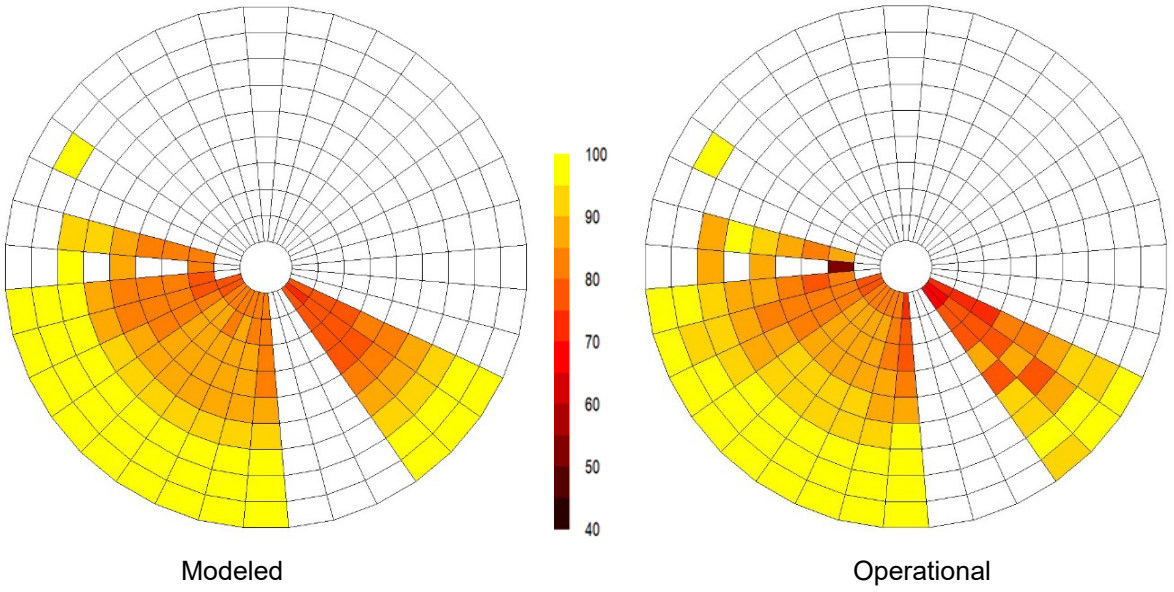

Figure 40: Onshore Site 11 mean array efficiency by speed and direction

The data used in this analysis represents around 24% of the total energy production and a zero mean error is given by a turbine roughness length of 3.5m.

8.1.12 Onshore Test Site 12

Onshore Test Site 12 is a larger wind farm with over 120 turbines. It is situated on flat terrain with an estimated background roughness of 0.04m.

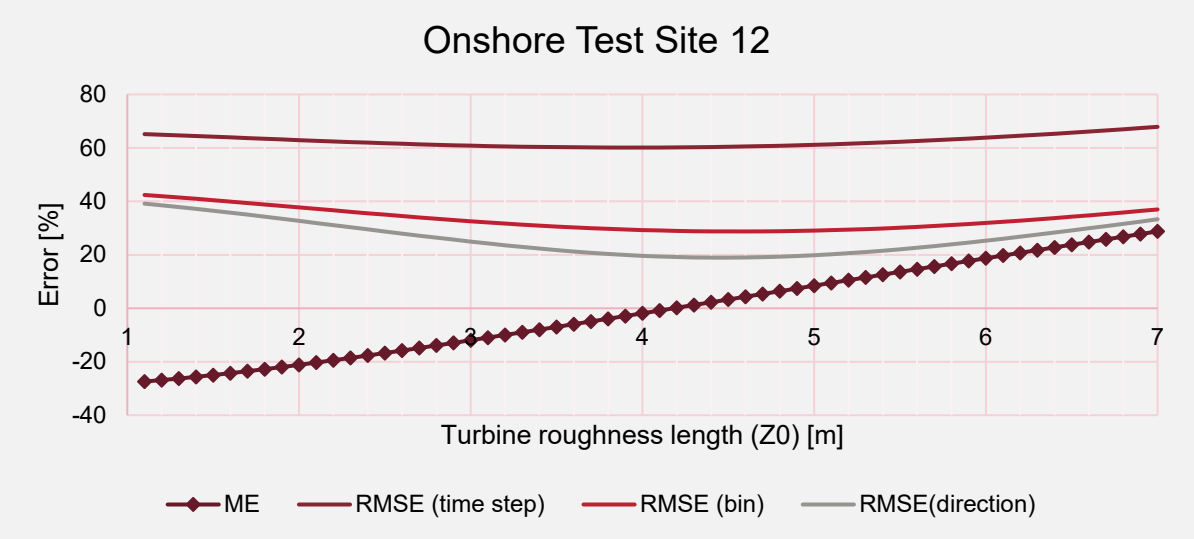

Figure 41: Onshore Site 12 variation in error metrics with turbine roughness

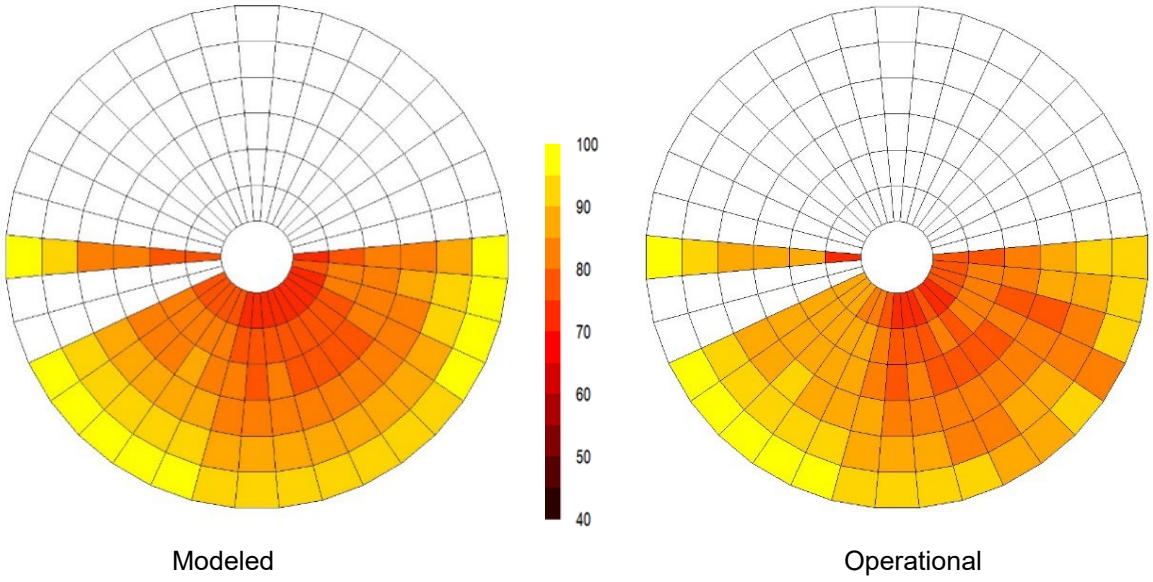

Figure 42: Onshore Site 12 mean array efficiency by speed and direction

Above, the innermost rings represent the 5m/s bin, while the outermost rings represent the 10m/s bin.

The data used in this analysis represents around 21% of the total energy production and a zero ME is given by a turbine roughness length of 4.2m.

8.1.13 Onshore Test Site 13

Onshore Test Site 13 is in flat terrain with an estimated background roughness length of between 0.07m and 0.15m. The project has several neighboring wind farms, making it a challenging to find unwaked directions.

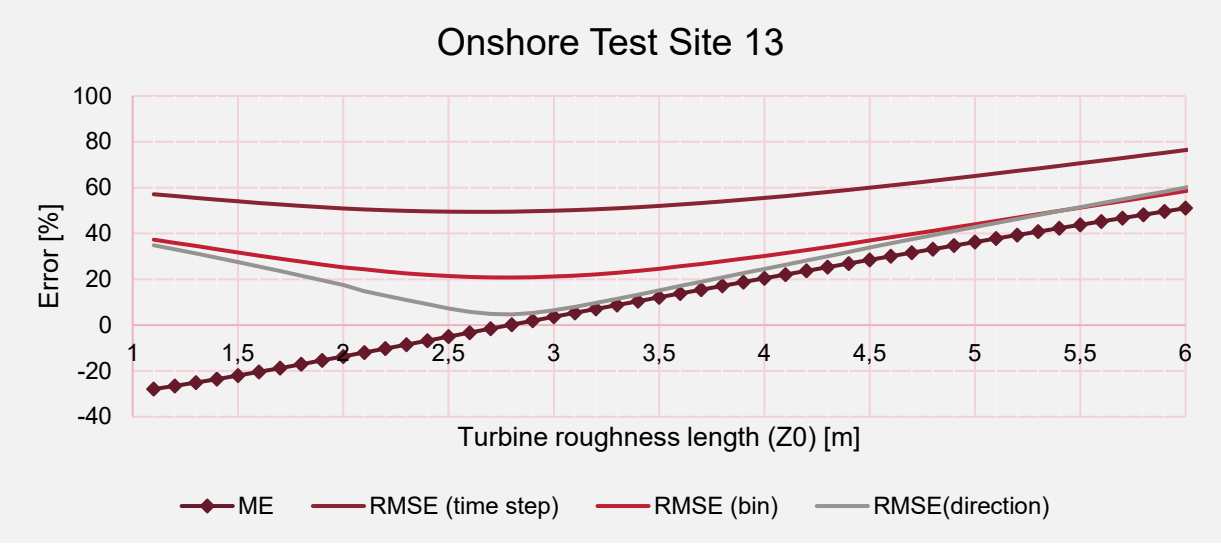

Figure 43: Onshore Site 13 variation in error metrics with turbine roughness

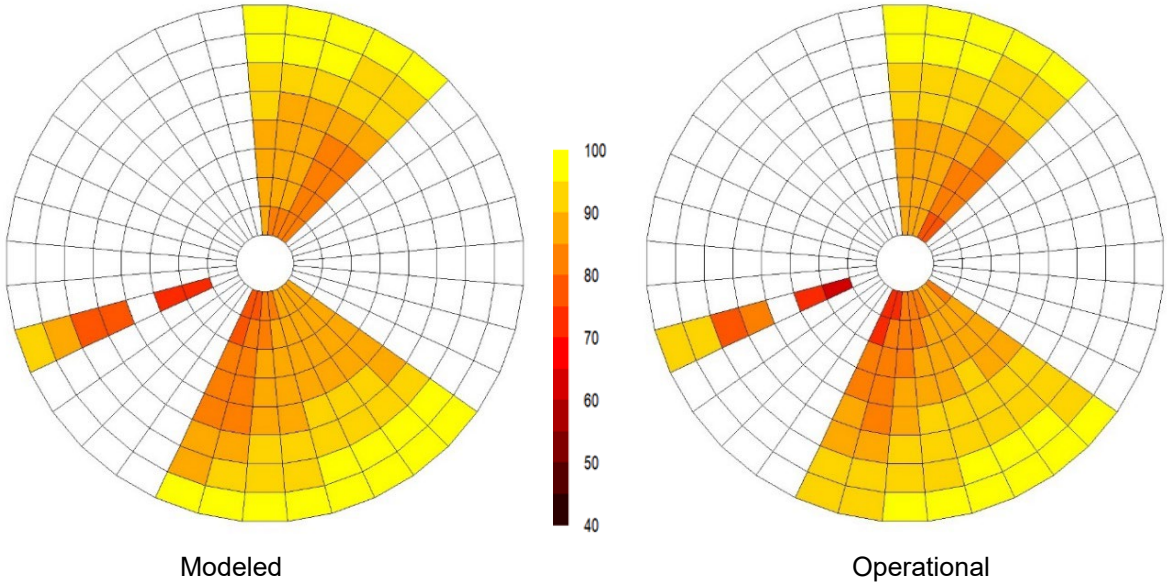

Figure 44: Onshore Site 13 mean array efficiency by speed and direction

Above, the innermost rings represent the 5m/s bin while the outermost rings represent the 12m/s bin.

The data used in this analysis represents around 13.5% of the total energy production and a zero ME is given by a turbine roughness length of 2.8m.

8.2 Onshore conclusions

All onshore test sites show variability in tuned turbine roughness and are representative of a wide range of wind farm configurations and environmental conditions. **Table 1** below summarizes the background roughness levels and the tuned turbine roughness from each site. Combining results for all onshore sites zero ME is achieved at a turbine roughness length of around 3.5m.

Onshore site	Background roughness length [m]	Tuned turbine roughness length [m]
1	0.07	2.2
2	0.07	2.8
3	0.07	2.5
4	0.05	6.0
5	0.05	5.3
6	0.07, 0.10	6.4
7	0.075	3.0
8	0.03	4.2
9	0.03, 0.05	1.7
10	0.05	3.5
11	0.07, 0.5	3.5
12	0.04	4.2
13	0.07, 0.15	2.8

Table 1: Tuned turbine roughness per site compared to background roughness length

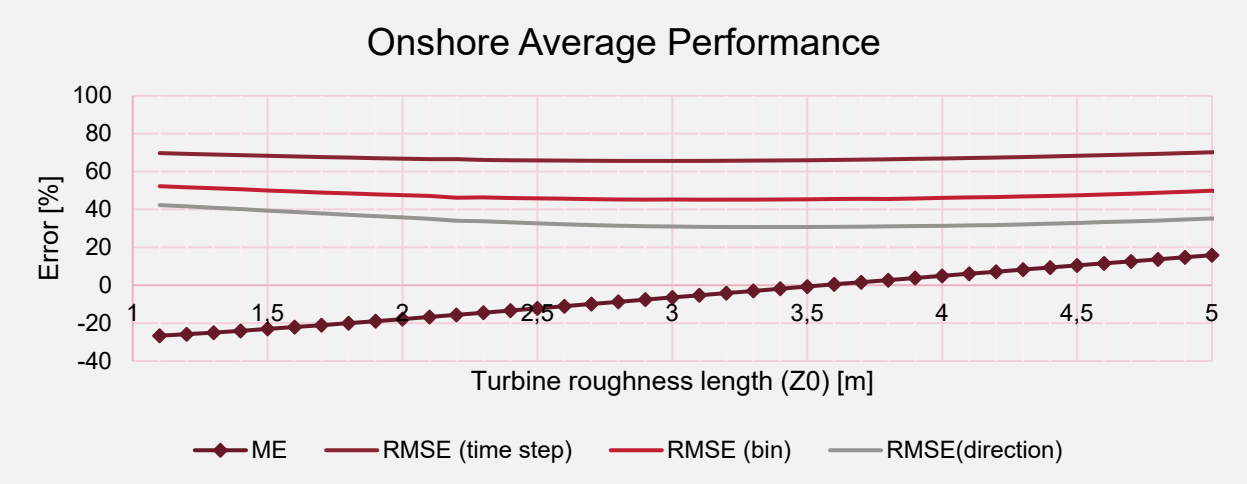

Figure 45: Onshore average variation in error metrics with turbine roughness

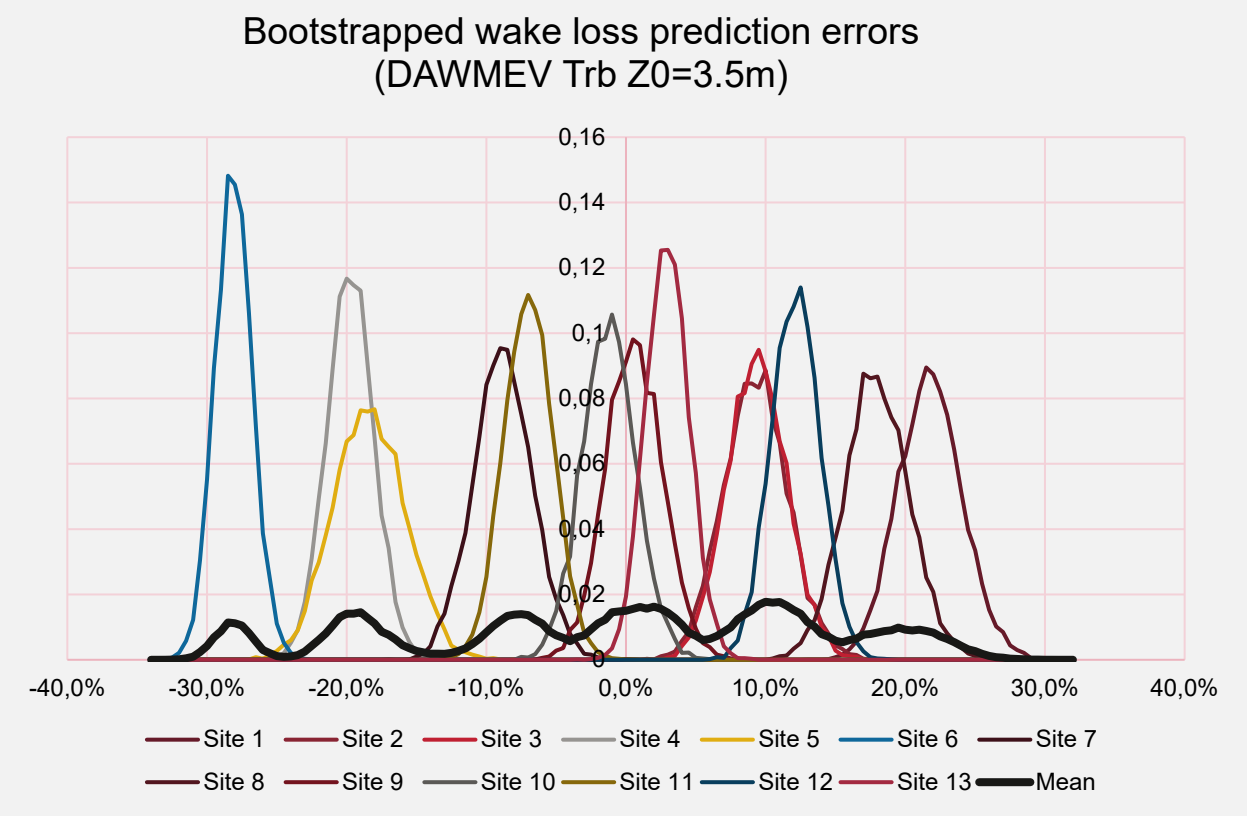

Figure 46: Bootstrapped errors for each site plus the combined errors across all 13 onshore sites

The combination of all 13 onshore sites with equal weighting gives a mean bias of -0.7% with a standard deviation of 14.8%. This represents a slight underestimation of the wake losses but supports an estimate of wake loss uncertainty of 15%. Error percentages presented are relative to inferred array losses and not as a fraction of overall energy yield.

Similar to the offshore results, onshore findings are limited by a lack of true freestream measurements, or sufficient information to remove turbine underperformance. The quantification of a global blockage effect has not been directly possible though the RHB induction model has been applied to each site. The range of background or surface roughness levels in the onshore test sites is broad but lacks coverage in very low roughness or coastal sites.

These observations, coupled with the fact that we are not explicitly modeling a global blockage effect, encourages UL Solutions to adopt a somewhat conservative approach using a turbine roughness length of 3.5m coupled with the RHB induction model. UL Solutions considers this a reasonable and relatively unbiased approximation of total array effects and assumes an equivalent annual energy prediction uncertainty of 20%.

9. Summary

In summary, UL Solutions now recommends the DAWM EV wake model to be used with a turbine roughness of 1.5m for offshore and 3.5m for onshore sites and the RHB induction model to be enabled with linear-linear combination. UL Solutions further recommends a conservative estimate of 20% of wake losses continue to be used.

Acknowledgements

Thanks to Dr. Michael Brower who helped refine the initial DAWM EV and was responsible for writing the first version of this document, as well as deriving the theoretical basis of the Deep Array Wake Model.

Thanks to Shell for sharing data from Egmond An Zee, for their valuable collaboration and for allowing us to publish the results here.

Thanks to Orsted for running UL Solutions results and giving permission to share results of comparison to their operational data. Special thanks to Ewa Johansen who was instrumental in originating the methods behind Orsted's wake bench.

Appendix A

The following screenshot gives the recommended values for the deep array eddy viscosity wake model for the offshore cases.

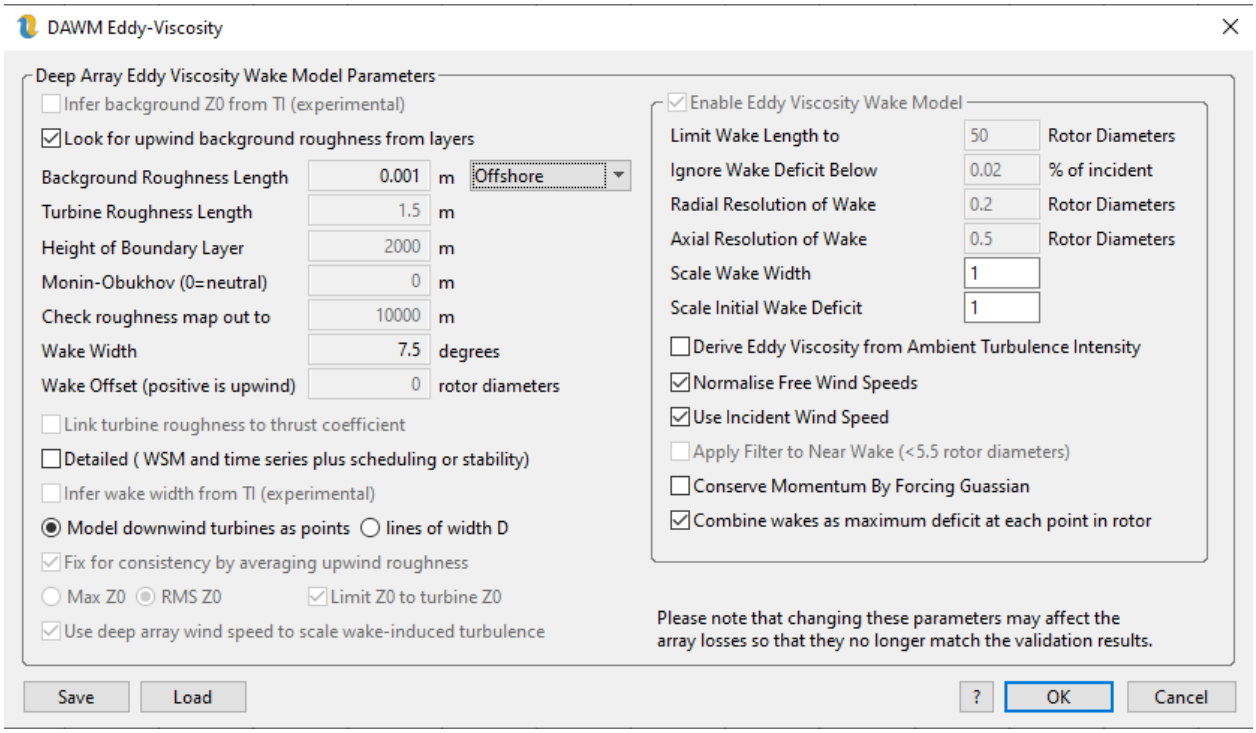

Figure 47: DAWM EV settings – offshore

The following screenshot gives the recommended values for the deep array eddy viscosity wake model for the onshore cases.

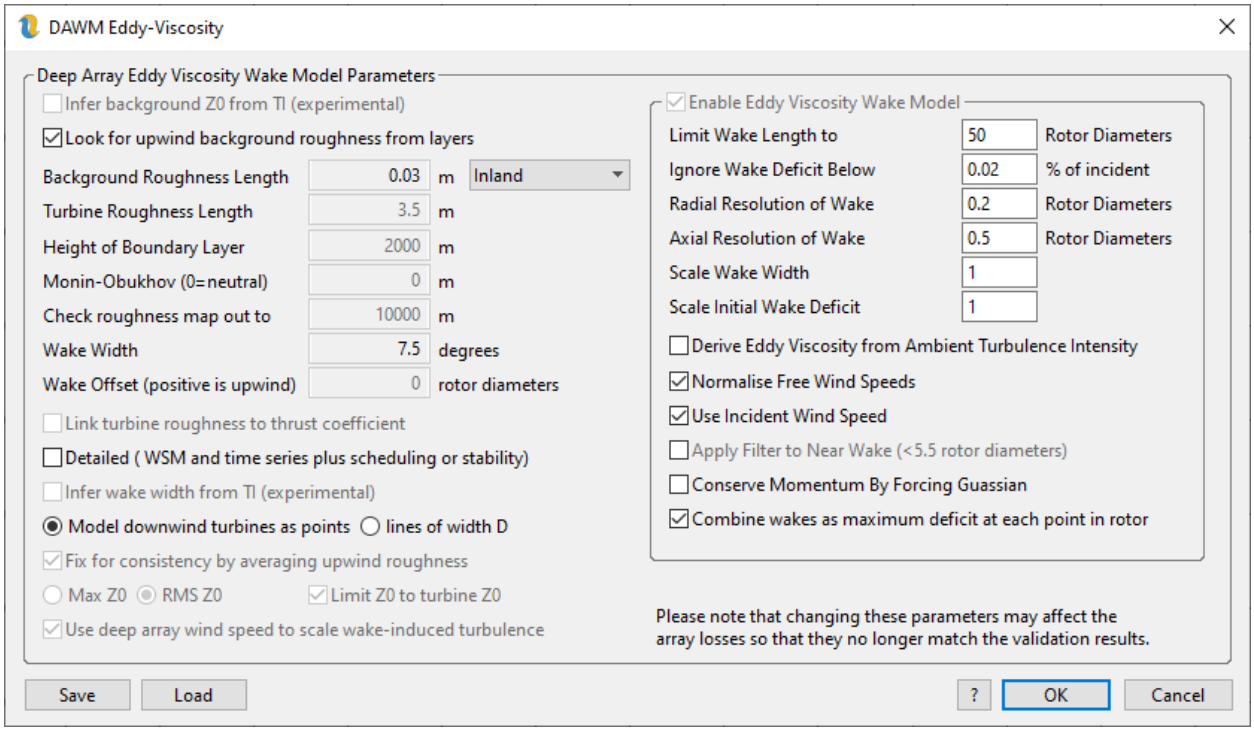

Figure 48: DAWM EV settings – onshore

The implementation of the Rankine Half-Body Induction model is shown below.

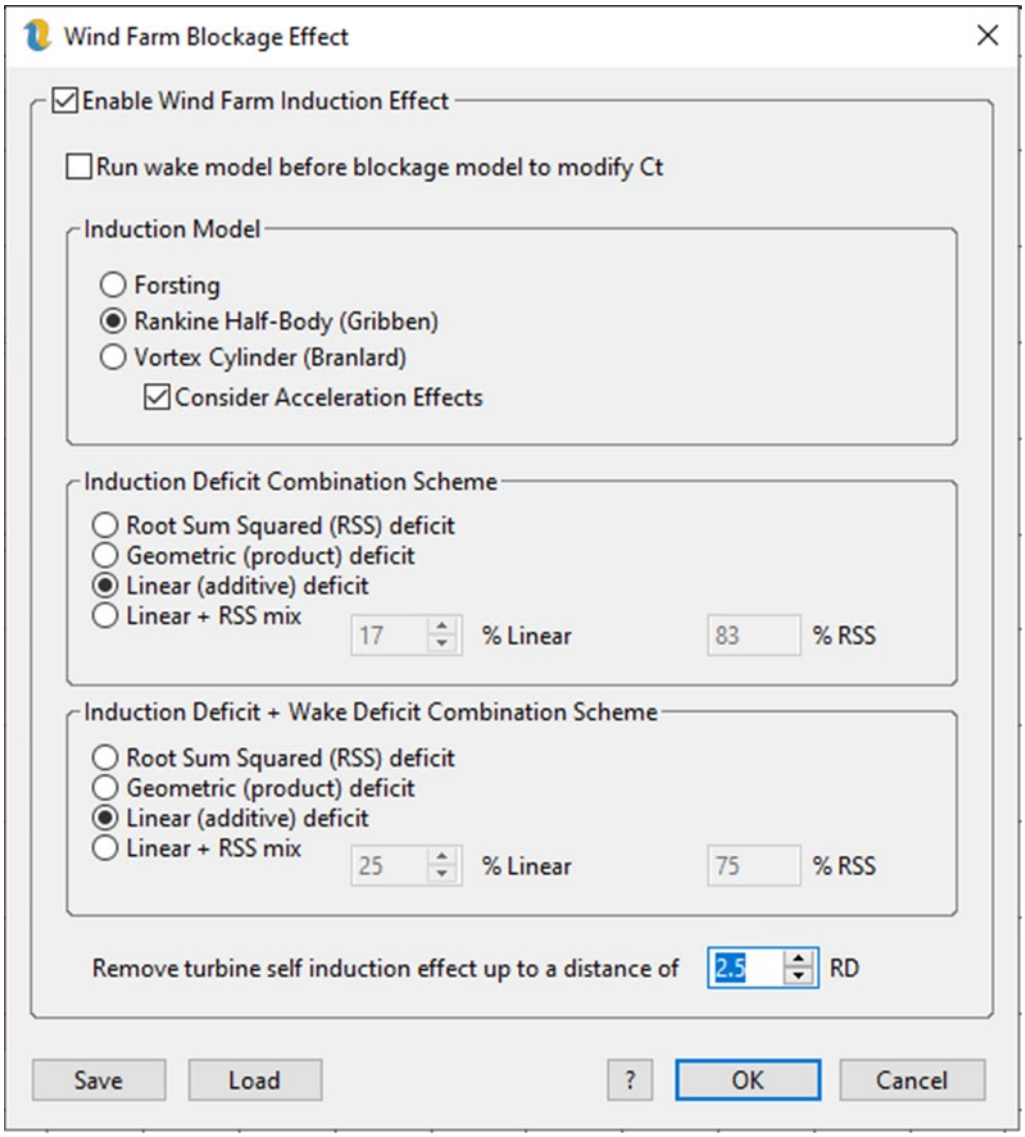

Figure 49: Rankine Half-Body Induction model settings

Safety. Science. Transformation.™